Journal of Porphyrins and Phthalocyanines
J. Porphyrins Phthalocyanines 2017; **21**: 1–20
DOI: 10.1142/S1088424617500389

Published at http://www.worldscinet.com/jpp/

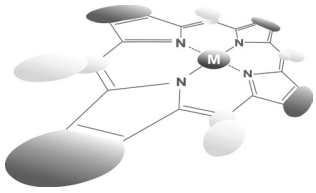

Discotic liquid crystals of transition metal complexes, 53†: synthesis and mesomorphism of phthalocyanines substituted by *m*-alkoxyphenylthio groups

Yoshiaki Chino[a], Kazuchika Ohta*[a◊], Mutsumi Kimura[b] and Mikio Yasutake[c]

[a] *Smart Material Science and Technology, Interdisciplinary Graduate School of Science and Technology, Shinshu University, 1-15-1 Tokida, Ueda, 386-8567, Japan*
[b] *Division of Chemistry and Materials, Faculty of Textile Science and Technology, Shinshu University, Ueda 386-8567, Japan*
[c] *Comprehensive Analysis Center for Science, Saitama University, 255 Shimo-Okubo, Sakura-Ku, Saitama 338-8570, Japan*

Received 5 March 2017
Accepted 29 March 2017

ABSTRACT: We have successfully synthesized a series of novel octakis(*m*-alkoxyphenylthio) phthalocyaninato copper(II) complexes, (*m*-C_nOPhS)$_8$PcCu (n = 2, 4, 6, 8, 10, 12, 14, 16: **1b~1i**), by our developed method to reveal their mesomorphism. The phase transition behavior and mesophase structures have been established by using a polarizing optical microscope, a differential scanning calorimeter, and a temperature-dependent small angle X-ray diffractometer. Interestingly, the very short chain-substituted derivatives, (*m*-C_1OPhS)$_8$PcCu (**1a**) and (*m*-C_2OPhS)$_8$PCu (**1b**), show a hexagonal ordered columnar (Col_{ho}) mesophase, whereas each of the other longer-chain-substituted derivatives, (*m*-C_nOPhS)$_8$PcCu (n = 4~16: **1c~1i**), shows only rectangular ordered columnar (Col_{ro}) mesophase(s). In contrast to the present longer-chain-substituted *phenylthio* derivatives, each of the previous longer-chain-substituted *phenoxy* derivatives, (*m*-C_nOPhO)$_8$PcCu (n = 10–20), shows a different columnar mesophase of Col_{ho}. We discuss this difference of mesomorphism from the viewpoint of the different steric hindrance originated by the peripheral substituents, PhO and PhS groups. Moreover, we could estimate the optical band gaps of (*m*-C_{10}OPhO)$_8$PcCu and (*m*-C_{10}OPhS)$_8$PcCu (**1f**) from absorption edge of the Q-bands to be 1.79 eV and 1.70 eV, respectively. Therefore, the *phenylthio*-substituted derivative gave a narrower band gap by *ca.* 0.1 eV in comparison with the *phenoxy*-substituted derivative.

KEYWORDS: phthalocyanine, metallomesogen, columnar mesophase, liquid crystals.

INTRODUCTION

Since the first discotic columnar liquid crystal was found by Chandrasekhar and co-workers in 1977 [1], various discogens have been synthesized up to date. In general, a columnar liquid crystal has a π-conjugated macrocyclic core such as triphenylene, hexabenzocoronene and phthalocyanine (Pc), together with more than six long alkyl chains in the periphery [2]. When these discogens are heated, the peripheral long alkyl chains firstly melt to form soft parts, but the central rigid cores maintain columnar stacking structure due to their strong π–π interaction. Accordingly, columnar liquid crystalline phases can be induced by this special situation. Therefore, pre-melting of the long alkyl chains by heating is driving force to induce liquid crystalline phases. In addition, since π orbitals of the π-conjugated macrocyclic cores are overlapped in one-dimensional columns formed by self-assembly, high charge carrier mobility along the columnar axis may be achieved. Therefore, the columnar liquid crystalline compounds exhibiting high charge carrier mobilities

◊ SPP full member in good standing

*Correspondence to: Kazuchika Ohta, email: ko52517@shinshu-u.ac.jp, tel/fax: +81 268-21-5492

† Part 52: Ref. 45 in this paper.

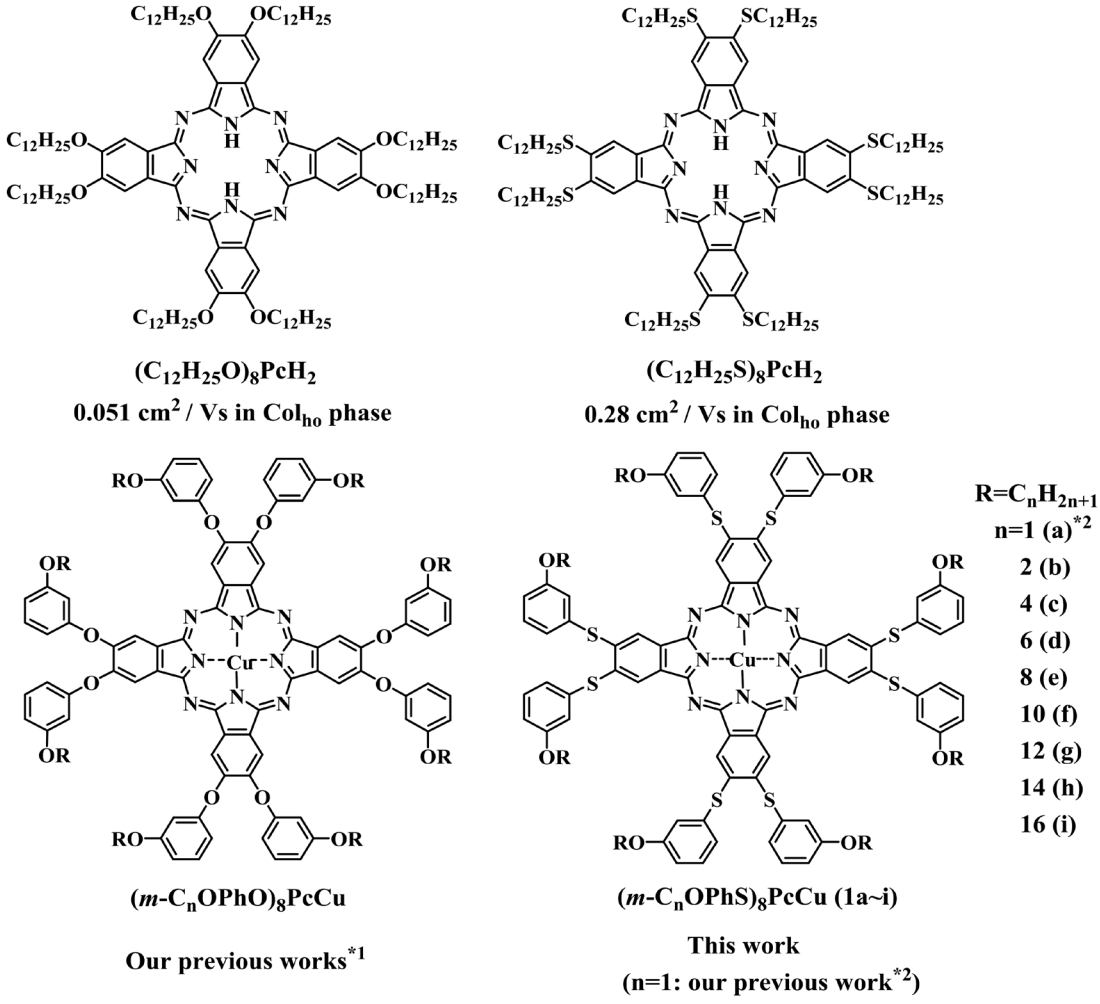

Fig. 1. Molecular formulae of liquid crystals based on phthalocyanine. *1: [8, 9, 21]. *2: [20]

have attracted a lot of our attention to apply to organic semiconducting devices such as organic photovoltaic cell, organic field effect transistor and so on [3]. In our previous works [4–6], we synthesized columnar liquid crystalline phthalocyanine compounds, $(C_{12}H_{25}O)_8PcH_2$ and $(C_{12}H_{25}S)_8PcH_2$, illustrated in Fig. 1. The hexagonal ordered columnar (Col_{ho}) phases in $(C_{12}H_{25}O)_8PcH_2$ and $(C_{12}H_{25}S)_8PcH_2$ exhibited high charge carrier mobilities of 0.051 cm^2/Vs and 0.28 cm^2/Vs, respectively. Therefore, the *alkylthio*(RS)-substituted phthalocyanine derivative gives about five times higher charge carrier mobility than the *alkoxy*(RO)-substituted phthalocyanine derivative. In order to achieve much higher charge carrier mobility in columnar liquid crystalline Pc compounds, the following two points may be furthermore required:

(1) to show very short intracolumnar stacking distance,
(2) to exhibit highly ordered alignment (ideally, homeotropic alignment).

In our previous works [7, 8], we found that substitution of *m*-alkoxyphenoxy (*m*-C_nOPhO) groups at the β-positions of Pc gave columnar liquid crystalline derivatives, (*m*-C_nOPhO)$_8$PcCu (Fig. 1), satisfying the above two requirements. Therefore, if we can synthesize columnar liquid crystalline phthalocyanines substituted by *m*-alkoxyphenylthio(*m*-C_nOPhS) groups instead of *m*-alkoxyphenoxy(*m*-C_nOPhO) groups, higher charge carrier mobility may be realized. The *alkylthio*-substituted phthalocyanine derivative, $(C_nS)_8PcH_2$, exhibits five times higher charge carrier mobility than the *alkoxy*-substituted phthalocyanine derivative, $(C_nO)_8PcH_2$, as mentioned above [4–6]. Therefore, we can expect similarly that the *phenylthio*-substituted derivative, $(PhS)_8PcCu$, may exhibit higher charge carrier mobility than the *phenoxy*-substituted derivative, $(PhO)_8PcCu$. Although the $(PhS)_8PcCu$ derivatives have been reported so far [9–19], no liquid crystalline $(PhS)_8PcCu$ derivatives have been reported.

Recently, we have synthesized $(PhS)_8PcCu$ complexes having very short methoxy groups at the *o-, m-, m-* & *p*-positions of the phenylthio group to induce mesomorphism in spite of the absence of long alkoxy chains [20]. The thermal fluctuation of the bulky substituents by heating makes soft parts to induce liquid crystalline

phases. Hence, they are categorized to "flying-seed-like" liquid crystals [21–25]. However, these flying-seed-like liquid crystals (x-$C_1OPhS)_8PcCu$ substituted by very short alkoxy groups are not suitable for application to organic semiconductor, because they show mesomorphism only at extremely high temperatures and transform into isotropic liquid with accompanying decomposition. Therefore, we have planned to synthesize new long *n*-alkoxy-substituted (m-$C_nOPhS)_8PcCu$ derivatives showing mesomorphism from room temperature and clearing into isotropic liquid without decomposition.

In this study, we have developed the synthetic route of the new *phenylthio*-substituted derivatives, (m-$C_nOPhS)_8PcCu$ (n = 2–16: **1b**–**1i** in Fig. 1), having long *n*-alkoxy groups at the *m*-position, in order to investigate their mesomorphism and mesomorphic structures. In comparison with the previous *phenoxy*-substituted Pc derivatives, (m-$C_nOPhO)_8$-PcCu (n = 10–20), we discuss the difference of mesomorphism from the viewpoint of the different steric hindrance originated by the peripheral PhO and PhS groups.

EXPERIMENTAL

Materials

The chemical reagents of 3-hydroxybenzenethiol, tritylchloride, Et_3SiH, 3-iodophenol, *n*-alkylbromide, $NaBH_4$ and 4,5-dichlorophthalonitrile were purchased from Tokyo Chemical Industry and used without further purifications. Other reagents were purchased from Wako Pure Chemical Industries and used without further purifications. Thin layer chromatography sheet (TLC) and silica gel were purchased from Merck. All reaction solvents were purchased from Wako Pure Chemical Industries. DMF was pre-dried over KOH and distilled over CaH_2 under reduced pressure and stored in the presence of 4A molecular sieves. THF was pre-dried over $CaCl_2$ and distilled from Na wire/benzophenone kethyl. 1-Hexanol was used without further purifications. Deuterated chloroform and DMSO for NMR measurements were purchased from Merck and WAKO Pure Chemical Industries, respectively. Abbreviations of reagents and solvents were as follows:

DBU: 1,8-diazabicyclo[5.4.0]-7-undecene, DMF: *N*,*N*-dimethylformamide, THF: tetrahydrofuran, DMSO: dimethylsulfoxid and TFA: trifluoroacetic acid.

Measurements

The ^1H NMR measurements were carried out by using a Bruker Ultrashield 400 MHz. The MALDI-TOF mass spectral measurements were carried out by using a Bruker Daltonics Autoflex III spectrometer (matrix: dithranol). The elemental analyses were performed by using a Perkin-Elmer Elemental Analyzer 2400. The data of MALDI-TOF mass spectra and elemental analyses are listed in Table 1. Electronic absorption (UV-vis) spectra were recorded by using a Hitachi U-4100 spectrophotometer. UV-vis spectral data of the (m-$C_nOPhS)_8PcCu$ complexes synthesized in this study were summarized in Table 2. Thermal gravimetric analysis (TGA) was carried out with a Rigaku Thermo Plus TG8120 thermal gravity analyzer. All TGA were performed under N_2 atmosphere. Phase transition behavior of the present complexes was observed with a polarizing optical microscope (Nikon ECLIPSE E600 POL; magnifications of the objective and ocular lenses were × 10, respectively) equipped with a Mettler FP82HT hot stage and a Mettler FP-90 Central Processor, and a Shimadzu DSC-50 differential scanning calorimeter. The phase transition temperatures and enthalpy changes are listed in Table 3. The mesophases were identified by using a small angle X-ray diffractometer (Bruker Mac SAXS System) equipped with a temperature-variable sample holder adopted a Mettler FP82HT hot stage.

Synthesis

Schemes 1 and 2 illustrate synthetic routes for the precursors of *m*-alkoxythiophenol (**4b~4i**) and the corresponding liquid crystalline Pc derivatives (m-$C_nOPhS)_8$-PcCu (**1b~1i**), respectively. All reactions were carried out under nitrogen atmosphere.

[*Route (a)*]

3-Triphenylmethylsulfanylphenol (2A). (Scheme 1) Synthetic method was adopted [26]. A three necked flask dried was charged with 3-hydroxybenzenethiol (1.03 g, 8.15 mmol) and dry pyridine (0.679 g, 8.58 mmol). Trityl chloride (2.27 g, 8.14 mmol) was added to the reaction mixture and it was stirred at rt for 3.5 h. When TLC (SiO_2/AcOEt:*n*-hexane = 1:1) confirmed disappearance of the spot of the starting reagent of 3-hydroxybenzenethiol (R_f = 0.50) and appearance of the target compound (R_f = 0.68), the reaction was terminated. The reaction mixture was diluted with water and extracted with dichloromethane. The organic layer was washed with water three times and saturated brine once. The organic layer was collected and dried over Na_2SO_4 overnight. Na_2SO_4 was filtrated off and dichloromethane and pyridine were evaporated *in vacuo*. The residue was dried *in vacuo* to obtain colorless oil (0.268 g). Yield 85.6%. ^1H NMR (400 MHz, d_6-DMSO, TMS): δ, ppm 9.31 (brs, 1H, -OH), 7.33–7.20 (m, 15H, ArH), 6.83 (t, J = 8.0 Hz, 1H, ArH), 6.55–6.52 (m, 1H, ArH), 6.39–6.38 (m, 1H, ArH), 6.32–6.30 (m, 1H, ArH).

1-Decyloxy-3-triphenylmethylsulfanylbenzene (3Af). (Scheme 1) Three necked flask dried was charged with 3-triphenylmethylsulfanylphenol (**2A**: 0.505 g, 1.37 mmol), Cs_2CO_3 (0.564 g, 1.73 mmol) and dry DMF (5 mL) at rt. 1-Bromodecane (0.315 g, 1.42 mmol) was added to the reaction mixture and stirred at rt for 4.5 h. When TLC (SiO_2/AcOEt:*n*-hexane = 1:1) confirmed disappearance of the spot of starting reagent (R_f = 0.18) of **2A** and appearance of the target compound (**3Af**) (R_f = 0.63), the reaction was terminated. The reaction

Table 1. Yields and elemental analysis data of (*m*-C_nOPhS)$_8$PcCu (**1a~1i**)

Compound	Mol. formula (Mol. wt)	Exact mass	Mass observed	Elemental analysis: Found (Calcd.) (%)			Yield (%)
				C	H	N	
1b: (*m*-C_2OPhS)$_8$PcCu	$C_{96}H_{80}N_8O_8S_8Cu$ (1793.77)	1791.32	1791.32	64.60 (64.28)	4.91 (4.50)	5.92 (6.25)	44.1
1c: (*m*-C_4OPhS)$_8$PcCu	$C_{112}H_{112}N_8O_8S_8Cu$ (2018.21)	2015.58	2015.50	66.30 (66.65)	5.74 (5.59)	5.47 (5.55)	65.9
1d: (*m*-C_6OPhS)$_8$PcCu	$C_{128}H_{144}N_8O_8S_8Cu$ (2242.64)	2239.83	2239.80	68.69 (68.55)	6.57 (6.47)	5.05 (5.00)	55.7
1e: (*m*-C_8OPhS)$_8$PcCu	$C_{144}H_{176}N_8O_8S_8Cu$ (2467.06)	2467.06	2464.14	69.97 (70.11)	7.31 (7.19)	4.81 (4.54)	60.4
1f: (*m*-C_{10}OPhS)$_8$PcCu	$C_{160}H_{208}N_8O_8S_8Cu$ (2691.49)	2688.33	2688.31	71.76 (71.40)	8.10 (7.79)	4.22 (4.16)	65.6
1g: (*m*-C_{12}OPhS)$_8$PcCu	$C_{176}H_{240}N_8O_8S_8Cu$ (2915.91)	2912.58	2913.61	72.47 (72.49)	8.53 (8.30)	3.59 (3.84)	68.1
1h: (*m*-C_{14}OPhS)$_8$PcCu	$C_{192}H_{272}N_8O_8S_8Cu$ (3140.34)	3136.83	3138.02	73.34 (73.43)	8.92 (8.73)	3.55 (3.57)	47.4
1i: (*m*-C_{16}OPhS)$_8$PcCu	$C_{208}H_{304}N_8O_8S_8Cu$ (3364.79)	3361.07	3362.24	74.07 (74.25)	9.42 (9.11)	3.23 (3.33)	66.1

Table 2. UV-vis spectral data in $CHCl_3$ solution of (m-C_nOPhO)$_8$PcCu (**1b~1i**)

Compound	Concentration ($X10^{-6}$mol L^{-1})	λ/nm (log ε)		
		Soret band	Q-band	
			Q_{0-1}-band	Q_{0-0}-band
1b: (m-C_2OPhS)$_8$PcCu	2.32	344.0 (4.91)	642.0 (4.68)	718.0 (5.42)
1c: (m-C_4OPhS)$_8$PcCu	2.39	344.0 (4.92)	642.0 (4.69)	716.0 (5.42)
1d: (m-C_6OPhS)$_8$PcCu	2.26	344.0 (4.93)	642.0 (4.69)	718.0 (5.43)
1e: (m-C_8OPhS)$_8$PcCu	2.26	344.0 (4.93)	642.0 (4.70)	718.0 (5.44)
1f: (m-C_{10}OPhS)$_8$PcCu	2.29	345.5 (4.90)	643.0 (4.65)	718.9 (5.42)
1g: (m-C_{12}OPhS)$_8$PcCu	2.42	342.0 (4.88)	642.0 (4.66)	718.0 (5.40)
1h: (m-C_{14}OPhS)$_8$PcCu	2.34	344.0 (4.88)	642.0 (4.65)	718.0 (5.38)
1i: (m-C_{16}OPhS)$_8$PcCu	2.37	344.0 (4.89)	642.0 (4.65)	718.0 (5.38)

Table 3. Phase transition temperatures and enthalpy changes of **1b~1i**

Compound	Phase T (°C) [ΔH (kJ.mol^{-1})] Phase ⇝ Relaxation
1a*: (m-C_1OPhS)$_8$PcCu	K_1 —ca. 180⇝ K_2 —287.4[15.8]→ Col_{ho} —334.2[6.7]→ I.L. (decomp.)
1b: (m-C_2OPhS)$_8$PcCu	K_v ⇄ 212.5[57.6] ⇄ Col_{ho} ⇄ 239.5[6.1] ⇄ I.L.
1c: (m-C_4OPhS)$_8$PcCu	K_v ⇄ 191.3 ⇄ Col_{ro2} (P2m) ⇄ 199.9 ⇄ I.L.
1d: (m-C_6OPhS)$_8$PcCu	K_{1v} —95.0[7.2]→ K_2 ⇄ 143.9[1.9] ⇄ Col_{ro2} (P2m) ⇄ 152.7[60.3] ⇄ I.L.
1e: (m-C_8OPhS)$_8$PcCu	K_{1v} ⇄ 106.5 ⇄ Col_{ro2} (P2m) ⇄ 142.6[60.3] ⇄ I.L.; K_{2v} ⇄ 100.1 ⇄; K_{3v} ⇄ 96.3 ⇄
1f: (m-C_{10}OPhS)$_8$PcCu	K_1 ⇄ 41.6[7.3] / 58.6[18.1] ⇄ K_{2v} ⇄ 64.7[3.2] ⇄ Col_{ro1} (P2m) ⇄ 81.1[7.5] ⇄ Col_{ro2} (P2m) ⇄ 133.5[95.5] ⇄ I.L.
1g: (m-C_{12}OPhS)$_8$PcCu	K_{2v} → Col_{ro1} (P2m) ⇝ K_1 ⇄ 81.5 ⇄ Col_{ro1} (P2m) ⇄ 98.5 ⇄ Col_{ro2} (P2m) ⇄ 110.9[67.0] ⇄ I.L.
1h: (m-C_{14}OPhS)$_8$PcCu	K_{2v} —55.0→ Col_{ro2} (P2m) ⇝ Col_{ro1} (P2m) ⇄ 93.2[6.5] ⇄ Col_{ro2} (P2m) ⇄ 117.9[70.9] ⇄ I.L.; K_{1v} —63.9→ ; K_{1v} —38.1 [4.1]→
1i: (m-C_{16}OPhS)$_8$PcCu	K_{1v} —75.0→ Col_{ro} (P2m) ⇄ 111.2[48.9] ⇄ I.L.; K_{2v} —64.0→

Phase nomenclature: K = crystal, Col_{ro} = rectangular ordered columnar, I.L. = isotropic liquid and v = virgin state. Col_{ro1}~Col_{ro2}: see Fig. 2. * [20].

mixture was diluted with water and extracted with dichloromethane. The organic layer was washed with water three times and saturated brine once. The organic layer was collected and dried over Na_2SO_4 overnight. Na_2SO_4 was filtrated off and dichloromethane was evaporated *in vacuo* to obtain the crude product. It was purified by silica gel column chromatography (R_f = 0.55, CH_2Cl_2:*n*-hexane = 1:2). The solvents were evaporated *in vacuo* and resulting product was dried *in vacuo* to obtain colorless oil (0.598 g). Yield 85.8%. ^{1}H NMR (400 MHz, d_6-DMSO, TMS): δ, ppm 7.35–7.21 (m, 15H, ArH), 6.98 (t, J = 7.9 Hz, 1H, ArH), 6.71, 6.70 (dd, J = 2.4, 6.0 Hz, 1H, ArH), 6.59 (d, J = 7.8 Hz, 1H, ArH), 6.32–6.31 (m, 1H, ArH), 3.58 (t, J = 6.6 Hz, 2H, -OCH_2-), 1.53 (quin,

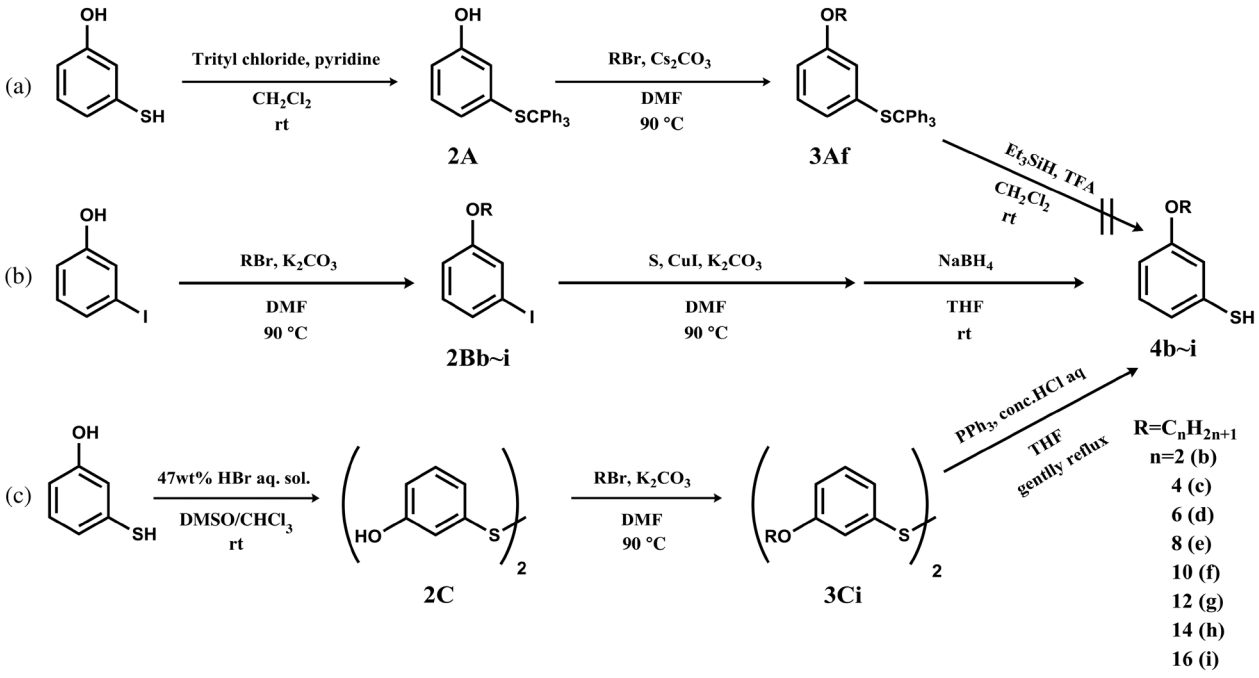

Scheme 1. Synthetic routes (a), (b) and (c) for 3-alkoxybenzenethiol: (a) by using the methods adopted [26] and [27]; (b) [30]; (c) [31]

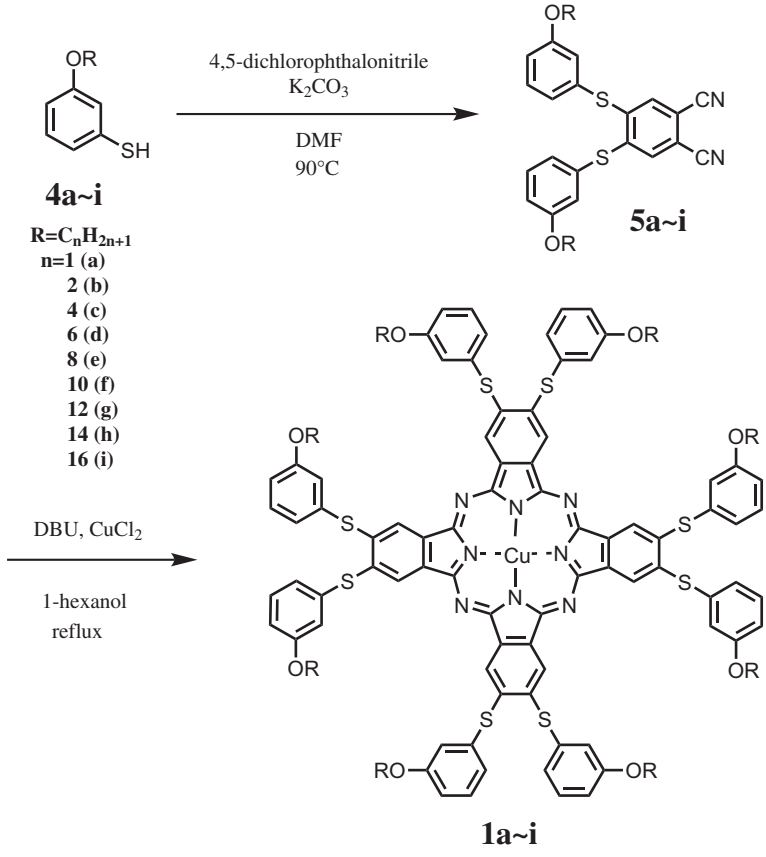

Scheme 2. Synthetic route for (*m*-C_nOPhS)$_8$PcCu (**1a~1i**). **1a**: previous work [20]

J = 6.4 Hz, 2H, -OCCH$_2$-), 1.32–1.20 (m, 14H, -CH$_2$- × 7), 0.857 (t, J = 6.7 Hz, 3H, -CH$_3$).

3-Decyloxybenzenethiol (4f). (Scheme 1) Synthetic method was adopted [27]. A three necked flask was charged with trifluoroacetic acid (3 mL), 1-decyloxy-3-triphenylmethylsulfanylbenzene (**3Af**: 0.598 g, 1.18 mmol), CH_2Cl_2 (1.1 mL) and Et_3SiH (0.487 g, 4.19 mmol). It was stirred at rt for 30 min. The reaction mixture was concentrated *in vacuo* and diluted with water and extracted with dichloromethane. The organic layer was washed with water three times and saturated brine once. The organic layer was collected and dried over Na_2SO_4 overnight. Na_2SO_4 was filtrated off and dichloromethane was evaporated *in vacuo*. Even by using any purification techniques, it was not possible to separate the target compound and the by-compound containing deprotection trityl group. Therefore, the synthesis of **4f** by Route A was abandoned. Next, synthesis of **4b~4i** by Route B in Scheme 1 was carried out.

[*Route* (*b*)]

3-Ethoxyiodobenzene (2Bb). (Scheme 1) A three necked flask dried was charged with K_2CO_3 (1.89 g, 13.7 mmol), 3-iodophenol (1.00 g, 4.55 mmol) and dry DMF (5 mL). Ethylbromide (0.595 g, 5.46 mmol) was then added to the reaction mixture and it was stirred at 90 °C. Proceeding of the reaction was monitored by TLC (SiO_2/*n*-hexane). After 1 h, disappearance of the spot of 3-iodophenol (R_f = 0.0) was confirmed, so that the reaction was quenched with water and cooled to rt. The product was extracted with ethyl acetate and the organic layer was washed with water three times and saturated brine once. The organic layer was collected and dried over Na_2SO_4 overnight. Na_2SO_4 was filtrated off and the solvent was evaporated *in vacuo* to obtain yellowish liquid (1.06 g). Yield 93.8%. The product was used for the next reaction without further purification. ^{1}H NMR (400 MHz, $CDCl_3$, TMS): δ, ppm 7.27–7.24 (m, 2H, ArH), 6.98 (t, J = 8.0 Hz, 1H, ArH), 6.86–6.84 (m, J = 2.4 Hz, 8.4 Hz, 1H, ArH), 4.00 (quart, J = 6.9 Hz, 2H, -OCH$_2$-), 1.40 (t, J = 7.0 Hz, 3H, -CH$_3$).

3-Hexyloxyiodobenzene (2Bd). Yield 91.6%. This synthesis was carried out as the same method of **2Bb**. The crude product was purified by silica gel column chromatography (*n*-hexane/R_f = 0.30) to obtain colorless liquid (1.29 g). ^{1}H NMR (400 MHz, $CDCl_3$, TMS): δ, ppm 7.20–7.18 (m, 2H, ArH), 6.90 (t, J = 7.8 Hz, 1H, ArH), 6.79–6.77 (m, 1H, ArH), 3.84 (t, J = 6.6 Hz, 2H, -OCH$_2$-), 1.69 (quin, J = 7.0 Hz, 2H, -OCC$\underline{H}_2$-), 1.41–1.22 (m, 6H, -(CH$_2$)$_3$-), 0.835 (t, J = 7.0 Hz, 3H, -CH$_3$). ^{1}H NMR datum was in accordance with Ref. 28.

Other homologs **2Bc~2i** were synthesized by the same method for **2Bd**. Only the yield and ^{1}H NMR data were shown below. All compounds were obtained as liquid except for **2Bi**.

3-Butoxyiodobenzene (2Bc). Yield 42.7%. ^{1}H NMR (400 MHz, $CDCl_3$, TMS): δ, ppm 7.27–7.25 (m, 2H, ArH), 6.98 (t, J = 8.0 Hz, 1H, ArH), 6.87–6.84 (m, 1H, ArH), 3.92 (t, J = 6.4 Hz, 2H, -OCH$_2$-), 1.75 (quin, J = 7.0 Hz, 2H, -OCC$\underline{H}_2$-), 1.48 (sext, J = 7.4 Hz, 2H, -OCCC$\underline{H}_2$-), 0.969 (t, J = 7.2 Hz, 3H, -CH$_3$).

3-Octyloxyiodobenzene (2Be). Yield 92.2%. ^{1}H NMR (400 MHz, $CDCl_3$, TMS): δ, ppm 7.20–7.17 (m, 2H, ArH), 6.91 (t, J = 7.8 Hz, 1H, ArH), 6.79–6.77 (m, 1H, ArH), 3.84 (t, J = 6.6 Hz, 2H, -OCH$_2$-), 1.69 (quin, J = 7.2 Hz, 2H, -OCC$\underline{H}_2$-), 1.40–1.20 (m, 10H, -(CH$_2$)$_5$-), 0.818 (t, J = 7.0 Hz, 3H, -CH$_3$). The ^{1}H NMR datum was in accordance with Ref. 29.

3-Decyloxyiodobenzene (2Bf). Yield 93.9%. ^{1}H NMR (400 MHz, $CDCl_3$, TMS): δ, ppm 7.30–7.27 (m, 2H, ArH), 7.04 (t, J = 8.2 Hz, 1H, ArH), 6.89–6.87 (m, 1H, ArH), 3.97 (t, J = 6.4 Hz, 2H, -OCH$_2$-), 1.85 (quin, J = 6.6 Hz, 2H, -OCC$\underline{H}_2$-), 1.50–1.30 (m, 14H, -(CH$_2$)$_7$-), 0.946 (t, J = 7.0 Hz, 3H, -CH$_3$).

3-Dodecyloxyiodobenzene (2Bg). Yield 85.2%. ^{1}H NMR (400 MHz, $CDCl_3$, TMS): δ, ppm 7.26–7.24 (m, 2H, ArH), 6.97 (t, J = 7.8 Hz, 1H, ArH), 6.86–6.83 (m, 1H, ArH), 3.91 (t, J = 6.6 Hz, 2H, -OCH$_2$-), 1.75 (quin, J = 7.0 Hz, 2H, -OCC$\underline{H}_2$-), 1.45–1.27 (m, 18H, -(CH$_2$)$_9$-), 0.881 (t, J = 7.0 Hz, 3H, -CH$_3$).

3-Tetradecyloxyiodobenzene (2Bh). Yield 84.1%. ^{1}H NMR (400 MHz, $CDCl_3$, TMS): δ, ppm 7.27–7.24 (m, 2H, ArH), 6.97 (t, J = 8.0 Hz, 1H, ArH), 6.86–6.84 (m, 1H, ArH), 3.91 (t, J = 6.4 Hz, 2H, -OCH$_2$-), 1.75 (quin, J = 6.6 Hz, 2H, -OCC$\underline{H}_2$-), 1.47–1.26 (m, 22H, -(CH$_2$)$_{11}$-), 0.88 (t, J = 7.0 Hz, 3H, -CH$_3$).

3-Hexadecyloxyiodobenzene (2Bi). Yield 83.3%, mp 32.4 °C. ^{1}H NMR (400MH, $CDCl_3$, TMS): δ, ppm 7.27–7.23 (m, 2H, ArH)), 6.98 (t, J = 8.0 Hz, 1H, ArH), 6.86–6.83 (m,1H, ArH), 3.91 (t, J = 6.6 Hz, 2H, -OCH$_2$-), 1.76 (quin, J = 7.0 Hz, 2H, -OCCH$_2$-), 1.43 (quin, J = 7.3 Hz, 2H, -OCCCH$_2$-), 1.33–1.26 (m, 24H, -CH$_2$- × 12), 0.88 (t, J = 6.8 Hz, 3H,-CH$_3$).

3-Ethoxybenzenthiol (4b). (Scheme 1) Synthetic method was adopted [30]. A three necked flask dried was charged with K_2CO_3 (1.00 g, 7.26 mmol), powdered sulfur (0.358 g, 11.2 mmol), CuI (72.3 mg, 0.380 mmol), 3-ethoxyiodebenzene (**2Bb**) (0.897 g, 3.62 mmol) and dry DMF (4 mL). The reaction was carried out at 90 °C with stirring for 12 h. TLC (SiO_2/*n*-hexane) confirmed disappearance of the spot of starting reagent of **2Bb** (Rf = 0.30) and appearance of the new spot (Rf = 0.0) were confirmed by TLC. The reaction mixture was cooled to rt and diluted with water. The product was extracted with ethyl acetate and the organic layer was washed with water three times and saturated brine once. The organic layer was collected and dried over Na_2SO_4 overnight. Na_2SO_4 was filtrated off and the solvent was evaporated *in vacuo* to obtain the crude product, which was used for next reaction without further purification. The three necked flask containing the crude product was charged with $NaBH_4$ (4.24 g, 112 mmol) and dry THF (10 mL) and it was stirred for 32 h. The reaction was quenched with slowly dropwise adding conc. HCl in an ice bath. The product was extracted with ethyl acetate and the organic

layer was washed with water three times and saturated brine once. The organic layer was collected and dried over Na_2SO_4 overnight. Na_2SO_4 was filtrated off and the solvent was evaporated *in vacuo* to obtain colorless liquid (0.382 g). The product was used for next reaction without further purifications. Yield 68.5%. ^{1}H NMR (400 MHz, $CDCl_3$, TMS): δ, ppm 7.12 (t, J = 8.0 Hz, 1H, ArH), 6.84–6.81 (m, 2H, ArH), 6.68 (dd, J = 2.0 Hz, 6.0 Hz, 1H, ArH), 4.00 (quart, J = 7.1 Hz, 2H, -OCH_2-), 3.44 (s, 1H, -SH), 1.39 (t, J = 7.0 Hz, 3H, -CH_3).

Other homologs **4c~4i** were synthesized by the same method for **4b**. Only the yield and ^{1}H NMR data were shown below. All compounds **4c~4i** were obtained as liquid.

3-Butoxybenzenethiol (4c). Yield 77.9%. ^{1}H NMR (400 MHz, $CDCl_3$, TMS): δ, ppm 7.12 (t, J = 8.0 Hz, 1H, ArH), 6.84–6.81 (m, 2H, ArH), 6.68 (dd, J = 3.2 Hz, 7.6 Hz, 1H, ArH), 3.93 (t, J = 6.4 Hz, 2H, -OCH_2-), 3.43 (s, 1H, -SH), 1.75 (quin, J = 7.0 Hz, 2H, -$OCCH_2$-), 1.48 (sext, J = 7.4 Hz, 2H, -$OCCCH_2$-), 0.969 (t, J = 7.4 Hz, 3H, -CH_3).

3-Hexyloxybenzenethiol (4d). Yield 65.9%. ^{1}H NMR (400 MHz, $CDCl_3$, TMS): δ, ppm 7.05 (t, J = 7.8 Hz, 1H, ArH), 6.76–6.75 (m, 2H, ArH), 6.62–6.60 (m, 1H, ArH), 3.86 (t, J = 6.6 Hz, 2H, -OCH_2-), 3.36 (s, 1H, -SH), 1.68 (quin, J = 7.1 Hz, 2H, -$OCCH_2$-), 1.41–1.27 (m, 6H, -$OCCCH_2$-), 0.832 (t, J = 6.8 Hz, 3H, -CH_3).

3-Octyloxybenzenethiol (4e). Yield 91.6%. ^{1}H NMR (400 MHz, $CDCl_3$, TMS): δ, ppm 7.05 (t, J = 8.0 Hz, 1H, ArH), 6.76–6.74 (m, 2H, ArH), 6.63–6.60 (m, 1H, ArH), 3.84 (t, J = 6.6 Hz, 2H, -OCH_2-), 3.36 (s, 1H, -SH), 1.69 (quin, J = 7.2 Hz, 2H, -$OCCH_2$-), 1.40-1.22 (m, 10H, $CH_2 \times 5$), 0.816 (t, J = 7.0 Hz, 3H, -CH_3).

3-Decyloxybenzenethiol (4f). Yield 80.5%. ^{1}H NMR (400 MHz, $CDCl_3$, TMS): δ, ppm 7.04 (t, J = 8.0 Hz, 1H, ArH), 6.79–6.73 (m, 2H, ArH), 6.63–6.59 (m, 1H, ArH), 3.84 (t, J = 6.6 Hz, 2H, -OCH_2-), 3.36 (s, 1H, -SH), 1.75 (quin, J = 7.0 Hz, 2H, -$OCCH_2$-), 1.41–1.20 (m, 14H, $CH_2 \times 7$), 0.811 (t, J = 6.8 Hz, 3H, -CH_3).

3-Dodecyloxybenzenethiol (4g). Yield 62.3%. ^{1}H NMR (400 MHz, $CDCl_3$, TMS): δ, ppm 7.12 (t, J = 8.2 Hz, 1H, ArH), 6.84–6.81 (m, 2H, ArH), 6.70–6.67 (m, 1H, ArH), 3.91 (t, J = 6.6 Hz, 2H, -OCH_2-), 3.43 (s, 1H, -SH), 1.76 (quin, J = 7.0 Hz, 2H, -$OCCH_2$-), 1.45–1.27 (m, 18H, $CH_2 \times 9$), 0.881 (t, J = 7.0 Hz, 3H, -CH_3).

3-Tetradecyloxybenzenethiol (4h). Yield 92.7%. ^{1}H NMR (400 MHz, $CDCl_3$, TMS): δ, ppm 7.12 (t, J = 7.8 Hz, 1H, ArH), 6.84–6.81 (m, 2H, ArH), 6.70–6.67 (m, 1H, ArH), 3.92 (t, J = 6.6 Hz, 2H, -OCH_2-), 3.43 (s, 1H, -SH), 1.76 (quin, J = 7.0 Hz, 2H, -$OCCH_2$-), 1.47–1.26 (m, 22H, $CH_2 \times 11$), 0.88 (t, J = 6.8 Hz, 3H, -CH_3).

3-Hexadecyloxybenzenethiol (4i). Yield 51.8%. ^{1}H NMR (400 MHz, $CDCl_3$, TMS): δ, ppm 7.12 (t, J = 8.2 Hz, 1H, ArH), 6.84–6.81 (m, 2H, ArH), 6.69, 6.68 (dd, J = 2.0 Hz, 6.0 Hz, 1H, ArH), 3.92 (t, J = 6.6 Hz, 2H, -OCH_2-), 3.44 (s, 1H, -SH), 1.76 (quin, J = 7.0 Hz, 2H, -$OCCH_2$-), 1.47–1.26 (m, 26H, -$(CH_2)_{13}$-), 0.88 (t, J = 6.4 Hz, 3H, -CH_3).

[*Route* (*c*)]

Derivative **4i** was also synthesized by another method, see Refs. 31 and 32.

Bis(3-hydroxyphenyl)disulfide (2C). (Scheme 1) In a three neck flask 3-hydroxybenzenethiol (0.247 g, 1.96 mmol) was dissolved in 10 mL of DMSO-$CHCl_3$ mixed solvent (1:1, v/v). To the reaction mixture, 47 wt% HBr aq. sol. (72.9 mg, 0.423 mmol) was added and it was stirred at rt for 12.5 h. When TLC (SiO_2/$CHCl_3$) confirmed disappearance of the spot of starting reagent of 3-hydroxybenzenethiol (R_f = 0.10) and appearance of a new spot of target compound **2C** (R_f = 0.0), the reaction was terminated. The solvents were evaporated *in vacuo* to concentrate the reaction mixture. The product was extracted with ethyl acetate and washed with water three times and saturated brine once. The organic layer was collected and dried over Na_2SO_4 overnight. Na_2SO_4 was filtrated off and the solvent was evaporated *in vacuo*. The residue was dried *in vacuo* to obtain the target compound **2C** as white powder (0.242 g). Yield 98.5%, mp 80–90 °C (broad). ^{1}H NMR (400 MHz, d_6-DMSO, TMS): δ, ppm 9.75 (s, 2H, -OH), 7.17 (t, J = 8.0 Hz, 2H, ArH), 6.93–6.90 (m, 4H, ArH), 6.68–6.60 (m, 2H, ArH).

Bis(3-hexadecyloxyphenyl) disulfide (3Ci). (Scheme 1) A three necked flask was charged with bis(3-hydroxyphenyl)disulfide (**2C**) (0.263 g, 1.05 mmol), K_2CO_3 (0.744 g, 5.38 mmol) and dry DMF (4 mL). 1-Bromohexadecane (0.808 g, 2.64 mmol) was then added to the reaction mixture and it was stirred at 90 °C for 3.5 h. The reaction was terminated when TLC (SiO_2/CH_2Cl_2) confirmed disappearance of both the spots of starting reagent of **2C** (Rf = 0.0) and monoalkylated compound (Rf = 0.55), and appearance of only one spot of dialkylated compound (SiO_2/CH_2Cl_2, Rf = 0.95). The reaction mixture was diluted with water and the product was extracted with dichloromethane. The organic layer was washed with water three times and saturated brine once. The organic layer was collected and dried over Na_2SO_4 overnight. Na_2SO_4 was filtrated off and the solvent was evaporated *in vacuo*. The crude product was recrystallised from acetone and then *n*-hexane at 25 °C to obtain white powder (0.330 g). Yield 44.9%, mp 62.5 °C (mp1), 64.8 °C (mp2). (This compound showed double melting behavior). ^{1}H NMR (400 MHz, $CDCl_3$, TMS): δ, ppm 7.18 (t, J = 8.2 Hz, ArH, 2H), 7.06–7.04 (m, ArH, 4H), 6.75, 6.74 (dd, J = 2.2 Hz, 6.6 Hz, ArH, 2H), 3.90 (t, J = 6.6 Hz, -(OCH_2)- × 2, 4H), 1.74 (quin, J = 7.1 Hz, -$(OCCH_2)$- × 2, 4H), 1.45–1.26 (m, -(CH_2)- × 26, 52H), 0.879 (t, J = 6.8 Hz, -CH_3 × 2, 6H).

3-Hexadecyloxybenzenthiol (4i). (Scheme 1) Compound **4i** was synthesized from compound **3Ci** according to the method used by authors in Ref. 32. A three necked flask was charged with bis(3-hexadecyloxypheny)disulfide (**3Ci**: 0.324 g, 0.464 mmol), PPh_3 (0.299 g, 1.14 mmol) and THF (12 mL) and then conc. HCl aq. sol. (0.4 mL) and H_2O (2 mL). It was gently refluxed with stirring for 5 h. After cooled to rt, large

excessive amounts of iodomethane was added to the reaction mixture and stirred at rt for 9 h. The reaction mixture was diluted with water and extracted with toluene. The organic layer was washed with water three times and saturated brine once. The organic layer was collected and dried over Na_2SO_4 overnight. Na_2SO_4 was filtrated off and the solvent was concentrated *in vacuo*. *n*-hexane was added to the solution until precipitation was occurred. It was heated until the precipitates were completely dissolved and then cooled to rt. The resulted precipitates were removed by filtration. To the filtrate *n*-hexane was furthermore added to occur precipitation completely. The precipitates were removed again by filtration, and then the filtrate was evaporated *in vacuo* to remove the solvent to afford colorless oil (0.151 g). Yield 46.5%. ^{1}H NMR (400 MHz, $CDCl_3$, TMS): δ, ppm 7.12 (t, J = 8.2 Hz, 1H, ArH), 6.84–6.81 (m, 2H, ArH), 6.69, 6.68 (dd, J = 2.0 Hz, 6.0 Hz, 1H, ArH), 3.92 (t, J = 6.6 Hz, 2H, -OCH_2-), 3.44 (s, 1H, -SH), 1.76 (quin, J = 7.0 Hz, 2H, -$OCCH_2$-), 1.47–1.26 (m, 26H, -$(CH_2)_{13}$-), 0.88 (t, J = 6.4 Hz, 3H, -CH_3).

4,5-Bis(*m*-ethoxyphenylthio)phthalonitrile (5b). Synthetic method was adopted [33]. A three necked flask was charged with K_2CO_3 (0.653 g, 4.73 mmol), 3-ethoxybenzenethiol (**3a**) (0.234 g, 1.52 mmol) and DMF (5 mL) and it was heated up to 90 °C. To the reaction mixture, 4,5-dichlorophthalonitrile (0.102 g, 0.517 mmol) was added and stirred at 90 °C for 7 h with occasionally monitoring by TLC. When the reaction was completed, it was quenched with water. The product was extracted with ethyl acetate and the organic layer was washed with water three times and saturated brine once. The organic layer was collected and dried over Na_2SO_4 overnight. Na_2SO_4 was filtrated off and the solvent was evaporated *in vacuo*. The crude product was purified by column chromatography (SiO_2, CH_2Cl_2, R_f = 0.50) to obtain white crystals (0.112 g). Yield 50.2%, mp 139.8 °C. ^{1}H NMR (400 MHz, $CDCl_3$, TMS): δ, ppm 7.41 (t, J = 8.2 Hz, 2H, ArH), 7.12–7.03 (m, 8H, ArH), 4.07 (quart, J = 7.1 Hz, 4H, -OCH_2-), 1.45 (t, J = 7.0 Hz, 6H, -CH_3).

Other homologs **5c~5i** were synthesized by the same method for **5b**. The eluents for the column chromatography, yields, melting points and ^{1}H NMR data were described below for these homologs.

4,5-Bis(*m*-butoxyphenylthio)phthalonitrile (5c). SiO_2, CH_2Cl_2:*n*-hexane = 4:1, R_f = 0.30. Yield 68.9%, mp 96.1 °C. ^{1}H NMR (400 MHz, $CDCl_3$, TMS): δ, ppm 7.41 (t, J = 7.4 Hz, 2H, ArH), 7.11–7.04 (m, 8H, ArH), 3.99 (t, J = 6.6 Hz, 4H, -OCH_2-), 1.80 (quin, J = 7.0 Hz, 4H, -$OCCH_2$-), 1.51 (sext, J = 7.5 Hz, 4H, -$OCCCH_2$-), 0.993 (t, J = 7.4 Hz, 6H, -CH_3).

4,5-Bis(*m*-hexyloxyphenylthio)phthalonitrile (5d). SiO_2, CH_2Cl_2:*n*-hexane = 4:1, R_f = 0.48. Yield 86.0%, mp 64.1°C. ^{1}H NMR (400 MHz, $CDCl_3$, TMS): δ, ppm 7.41 (t, J = 7.9 Hz, 2H, ArH), 7.11–7.03 (m, 8H, ArH), 3.98 (t, J = 6.4 Hz, 4H, -OCH_2-), 1.81 (quin, J = 7.0 Hz, 4H, -$OCCH_2$-), 1.49–1.33 (m, 12H, (-CH_2-)$_3$ × 2), 0.914 (t, J = 7.0 Hz, 6H, -CH_3).

4,5-Bis(*m*-octyloxyphenylthio)phthalonitrile (5e). SiO_2, CH_2Cl_2:*n*-hexane = 4:1, R_f = 0.58. Yield 95.1%, mp 72.1°C. ^{1}H NMR (400 MHz, $CDCl_3$, TMS): δ, ppm 7.41 (t, J = 8.0 Hz, 2H, ArH), 7.11–7.03 (m, 8H, ArH), 3.98 (t, J = 6.6 Hz, 4H, -OCH_2-), 1.81 (quin, J = 7.1 Hz, 4H, -$OCCH_2$-), 1.49–1.24 (m, 20H, (-CH_2-)$_5$ × 2), 0.889 (t, J = 6.8 Hz, 6H, -CH_3).

4,5-Bis(*m*-decyloxyphenylthio)phthalonitrile (5f). SiO_2, CH_2Cl_2, R_f = 0.80. Yield 78.1%, mp 76.5 °C. ^{1}H NMR (400 MHz, $CDCl_3$, TMS): δ, ppm 7.43 (t, J = 7.6 Hz, 2H, ArH), 7.13–7.08 (m, 8H, ArH), 4.00 (t, J = 6.6 Hz, 4H, -OCH_2-), 1.83 (quin, J = 7.4 Hz, 4H, -$OCCH_2$-), 1.53–1.31 (m, 28H, (-CH_2-)$_7$ × 2), 0.904 (t, J = 6.6 Hz, 6H, -CH_3).

4,5-Bis(*m*-dodecyloxyphenylthio)phthalonitrile (5g). SiO_2, CH_2Cl_2:*n*-hexane = 4:1, R_f = 0.58. Yield 29.3%, mp 76.2 °C. ^{1}H NMR (400 MHz, $CDCl_3$, TMS): δ, ppm 7.41 (t, J = 8.2 Hz, 2H, ArH), 7.11–7.03 (m, 8H, ArH), 3.98 (t, J = 6.6 Hz, 4H, -OCH_2-), 1.81 (quin, J = 7.1 Hz, 4H, -$OCCH_2$-), 1.50–1.21 (m, 36H, (-CH_2-)$_9$ × 2), 0.88 (t, J = 6.8 Hz, 6H, -CH_3).

4,5-Bis(*m*-tetradecyloxyphenylthio)phthalonitrile (5h). SiO_2, CH_2Cl_2:*n*-hexane = 4:1, R_f = 0.38. Yield 75.0%, mp 50.0 °C (mp_1), 83.3 °C (mp_2) (this compound showed double melting behavior). ^{1}H NMR (400 MHz, $CDCl_3$, TMS): δ, ppm 7.41 (t, J = 7.8 Hz, 2H, ArH), 7.11–7.04 (m, 8H, ArH), 3.98 (t, J = 6.4 Hz, 4H, -OCH_2-), 1.81 (quin, J = 7.0 Hz, 4H, -$OCCH_2$-), 1.49–1.26 (m, 44H (-CH_2-)$_{11}$ × 2), 0.879 (t, J = 6.8 Hz, 6H, -CH_3).

4,5-Bis(*m*-hexadecyloxyphenylthio)phthalonitrile (5i). SiO_2, CH_2Cl_2:*n*-hexane = 5:2, R_f = 0.70. Yield 73.9%, mp 58.3 °C (mp_1), 70.2 °C (mp_2) (this compound showed double melting behavior). ^{1}H NMR (400 MHz, $CDCl_3$, TMS): δ, ppm 7.41 (t, J = 8.2 Hz, 2H, ArH), 7.11–7.03 (m, 8H, ArH), 3.98 (t, J = 6.4 Hz, 4H, -OCH_2-), 1.81 (quin, J = 7.0 Hz, -$OCCH_2$-), 1.47 (quin, J = 7.2 Hz, -$OCCCH_2$-), 1.38–1.26 (m, 48H, -$(CH_2)_{12}$-,), 0.878 (t, J = 6.8 Hz, 6H, -CH_3).

Octakis(*m*-ethoxyphenylthio)phthalocyaninato copper(II) (1b). A three necked flask was charged with anhydrous $CuCl_2$ (15.5 mg, 0.115 mmol), 4,5-bis(3-ethoxyphenylthio)phthalonitrile (94.1 mg, 0.218 mmol) and 1-hexanol (5 mL). To the reaction mixture 5 drops of DBU was added and refluxed for 1.5 h. It was cooled to rt and poured into methanol to precipitate. The precipitates were collected by filtration and washed with methanol, ethanol and ethyl acetate successively. The precipitates were purified by Soxhlet extraction (toluene) two times. The obtained toluene solution was concentrated *in vacuo* and the residue was reprecipitated from acetone to obtain green solid (43.1 mg).

The homologs **1c**, **1h** and **1i** were also synthesized and purified by the same procedure for **1b**.

Octakis(*m*-hexyloxyphenylthio)phthalocyaninato copper(II) (1d). A three necked flask was charged with anhydrous $CuCl_2$ (9.2 mg, 0.068 mmol), 4,5-bis (3-hexyloxyphenylthio)phthalonitrile (**5d**: 48.2 mg,

0.0885 mmol) and 1-hexanol (5 mL). To the reaction mixture 5 drops of DBU was added and it was refluxed with stirring for 1.5 h. It was cooled to rt and poured into methanol to precipitate. The precipitates were collected by filtration and washed with methanol, ethanol and ethyl acetate successively. The residue was dissolved in chloroform and the solution was concentrated *in vacuo*. Subsequently, the crude product was purified by column chromatography (SiO_2, $CHCl_3$, Rf = 1.0) to obtain green solid (27.6 mg).

The homologs **1e~1g** were also synthesized and purified by the same procedure for **1d**. Table 1 lists the yields, MALDI-TOF-MASS and elemental analysis data of all the homologs **1b~1i**. The UV-vis spectral data were summarized in Table 2.

Decomposition temperatures of 1b~1i

Decomposition temperatures (T_d) obtained from TGA are listed below.

1b. T_d > 400 °C, **1c.** T_d = 389 °C, **1d.** T_d = 397 °C, **1e.** T_d = 359 °C, **1f.** T_d = 386 °C, **1g.** T_d = 399 °C, **1h.** T_d = 371 °C, **1i.** T_d = 360 °C.

RESULTS AND DISCUSSION

Synthesis

Phenylthio substituted phthalocyanine derivatives $(PhS)_8PcM$ (M = H_2, metal) reported up to date were prepared from commercially available benzenethiol derivatives as the starting reagents [10–20]. However, each of these benzenethiol derivatives does not have long alkyl chains. Therefore, at first we have developed the synthetic route for the long alkoxy chain-substituted benzenethiols **4b~4i** in this study. Although many synthetic methods for benzenethiol derivatives have been reported so far [34–39], we have tried in this study the following three relatively simple methods (Routes (a), (b) and (c) in Scheme 1) for the long alkoxy chain-substituted benzenethiol precursors **4b**–**4i**.

Route (a) in Scheme 1 was followed [26, 27]. The starting material, 3-hydroxybenzenethiol, was commercially available. The thiol group in 3-hydroxybenzenethiol was protected with trityl group to obtain derivative **2A**. Subsequently, the OH group in the phenol derivative **2A** was substituted by an alkoxy group using Williamson reaction to obtain derivative **3Af**. The trityl group in **3Af** was deprotected by triethylsilane in acidic condition. Although the reaction proceeded, it was not possible to separate the target compound **4f** and the by-product containing trityl group. It is attributable to the nonpolarity of both the target compound and the by-product having non-polar decyl groups. In Refs. 26 and 27, the target benzenethiol derivative can be separated from reaction mixture since substituent R is higher polarity group than decyloxy group. Due to the low polarity of substituent R in this study, Compound **4f** could not be separated from the reaction mixture.

Route (b) in Scheme 1 was followed [30]. Firstly, the OH group in 3-iodophenol was substituted by long alkoxy group using Williamson reaction to obtain derivatives **2Bb~2Bi**. Subsequently, these iodobenzene derivatives **2Bb~2Bi** were successfully converted into benzenethiol derivatives **4b~4i** in good yields (average total yield: 62.8%).

Derivative **4i** was also successfully synthesized by using another method [31] (Route (c) in Scheme 1). Firstly, commercially available 3-hydroxybenzenethiol was converted into corresponding disulfide derivative **2C** in the presence of HBr aq. sol. and DMSO. Subsequently, the OH groups in this disulfide derivative **2C** were substituted by long alkoxy groups using Williamson reaction to obtain disulfide derivative **3Ci**. Following the method used by authors in Ref. 32, derivative **3Ci** was converted into corresponding benzenethiol derivative **4i**. This method also successfully provided the key benzenethiol derivative **4i** in moderate yield (total yield: 20.1%).

Thus, the methods of Routes (b) and (c) in Scheme 1 successfully provided the long alkoxy-substituted benzenethiol derivatives **4b~4i**.

As shown in Scheme 2, the target phthalocyanine derivatives (m-C_nOPhS)$_8$PcCu (**1a~1i**) were synthesized using the method used by authors in Ref. 33. Firstly, each of the long alkoxy-substituted benzenethiol derivatives **4a~4i** was reacted with 4,5-dichlorophthalonitrile to obtain the phthalonitrile derivatives **5a~5i**. These phenylthio-substituted phthalonitriles **5a~5i** were tetracyclized to afford the target phenylthio-substituted phthalocyanines, (m-C_nOPhS)$_8$PcCu (**1a~1i**), in relatively good yields (average yield: 59%). Each of the phthalocyanines could be satisfactorily identified by the MALDI-TOF MASS, elemental analysis and UV-vis spectrum (Tables 1 and 2).

Phase transition behavior

Table 3 summarizes phase transition behavior of all the phenylthio-substituted PcCu complexes: the shortest-alkoxy-substituted derivative (m-C_1OPhS)$_8$PcCu (**1a**) synthesized in our previous work, and the other longer-alkoxy-substituted derivatives, (m-C_nOPhS)$_8$PcCu (n = 2~16; **1b~1i**), synthesized in this work.

In Fig. 2, the phase transition temperatures of all the derivatives (m-C_nOPhS)$_8$PcCu (n = 1~16: **1a~1i**) were plotted against the alkyl chain length (n). As can be seen this figure, each of the lines for the clearing points (○), the highest melting points (●), and the liquid crystal–liquid crystal transition points (▲) is very smoothly connected. However, there is only a gap between n = 2 and 4 for the melting points. It may correspond to the difference of mesomorphism driving forces between the

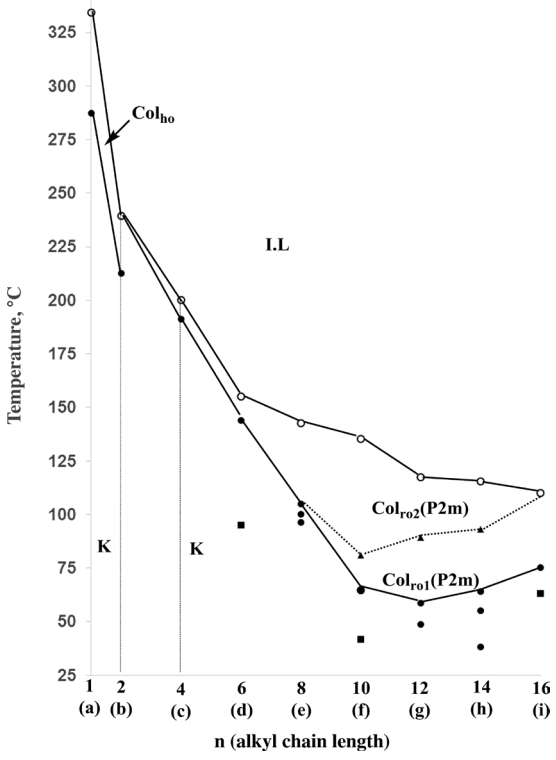

Fig. 2. Phase transition temperature *vs*. the number of carbon atom in the alkoxy chains for (*m*-C_nOPhS)$_8$PcCu (**1a**–**1i**). ○: clearing point, ●: melting point, ▪: crystal–crystal phase transition, and ▲: mesophase–mesophase transition

hexagonal ordered columnar (Col$_{ho}$) phases for **1a**–**1b** (n = 1, 2) and the rectangular ordered columnar (Col$_{ro}$ (P2m)) phases for **1c~1i** (n = 4~16). Furthermore, each of the derivatives **1f~1i** (n = 10~16) shows two rectangular ordered columnar phases of Col$_{ro1}$(P2m) and Col$_{ro2}$(P2m).

Interestingly, the Col$_{ho}$ phases appear only for the extremely short alkoxy-substituted derivatives **1a**–**1b** (n = 1, 2), so that these discogens can be considered as flying-seed-like liquid crystals induced by thermal fluctuation of the bulky peripheral substituents [20–25]. On the other hand, the Col$_{ro}$(P2m) phase(s) appear only for the longer alkoxy-substituted derivatives **1c~1i** (n = 4~16), so that these discogens can be considered as conventional liquid crystals induced by melting of the peripheral long alkoxy chains. To the best of our knowledge, this is the first example of changing from flying-seed-like liquid crystals to long alkyl chain type of liquid crystals in a series of liquid crystalline homologs.

Polarizing optical microscopic observation

Figure 3 shows the polarizing optical photomicrographs of liquid crystalline phases in the representative derivatives, **1b** (n = 2), **1f** (n = 10) and **1i** (n = 16). Both (a) and (b) are the photomicrographs of the liquid crystalline phase in the shortest alkoxy-substituted derivative (*m*-C_2OPhS)$_8$PcCu (**1b**) at 220 °C. As can be

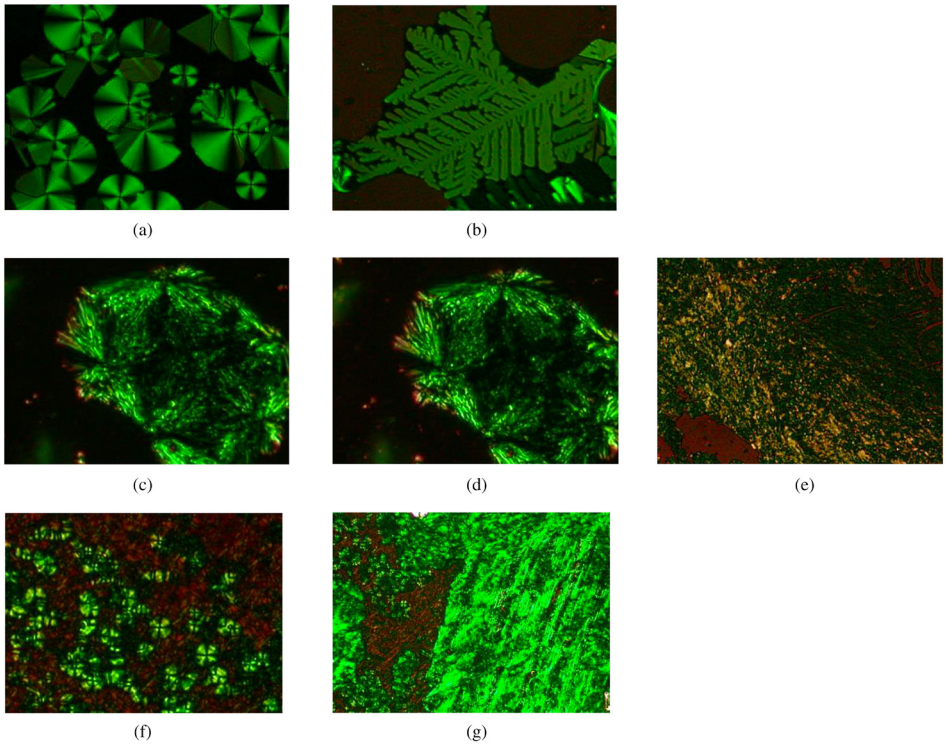

Fig. 3. Photomicrographs of (a) and (b): Col$_{ho}$ of (*m*-C_2OPhS)$_8$PcCu (**1b**) at 220 °C; (c) Col$_{ro2}$(P2m) of (*m*-C_{10}OPhS)$_8$PcCu (**1f**) at 115 °C; (d) Col$_{ro1}$(P2m) of (*m*-C_{10}OPhS)$_8$PcCu (**1f**) at 90 °C; (e) sheared sample of the photo (d) of **1f** at 90 °C; (f) Col$_{ro1}$(P2m) of (*m*-C_{16}OPhS)$_8$PcCu (**1i**) at 100 °C; (g) sheared sample of the photo (f) of **1i** at 100 °C

Table 4. X-ray data of **1a~1i**

Compound (mesophase)	Lattice constants/Å	Spacing/ Å		Miller indices (*h k l*)
		Observed	Calculated	
1a*: (*m*-C_1OPhS)$_8$PcCu				
Col_{ho} at 300 °C	*a* = 20.9	18.1	18.2	(1 0 0)
	h = 6.82	13.6	13.6	(0 0 1)^{2h}
	Z = 0.95 for ρ = 1.1	10.1	10.5	(1 1 0)
		9.16	9.05	(2 0 0)
		6.82	6.82	(0 0 1)^{h}
		ca. 5.9	6.03	(3 0 0) + #1
		3.98	3.95	(4 1 0)
1b: (*m*-C_2OPhS)$_8$PcCu				
Col_{ho} at 220 °C	*a* = 22.0	19.0	19.0	(1 0 0)
	h = 7.12	14.3	14.4	(0 0 1)^{2h}
	Z = 1.0 for ρ = 1.1	10.9	11.0	(1 1 0)
		7.12	7.19	(2 1 0) + (0 0 1)^{h}
		6.23	6.34	(3 0 0)
		ca. 5.2	—	#1
		4.00	4.15	(4 1 0)
1c: (*m*-C_4OPhS)$_8$PcCu				
Col_{ro2} (P2m) at 199 °C	*a* = 22.7	22.7	22.7	(1 0 0)
	b = 21.7	10.8	10.8	(0 2 0)
	h = 7.17	7.17	7.17	(0 0 1)^{h}
	Z = 1.1 for ρ = 1.0	5.26	5.27	(1 4 0)
		4.88	4.89	(2 4 0) + #1
		4.18	4.19	(5 2 0)
		3.71	3.73	(6 1 0)
1d: (*m*-C_6OPhS)$_8$PcCu				
Col_{ro2} (P2m) at 148 °C	*a* = 36.8	26.6	26.6	(0 1 0)
	b = 26.6	18.4	18.4	(2 0 0)
	h = 3.60	10.7	10.8	(2 2 0)
	Z = 1.0 for ρ = 1.1	8.61	8.63	(1 3 0)
		7.92	8.00	(2 3 0)
		5.82	5.85	(3 4 0)
		5.02	5.04	(6 3 0)
		4.58	4.60	(8 0 0) + #2
		4.06	4.08	(8 3 0)
		3.60	3.60	(0 0 1)^{h}
1e: (*m*-C_8OPhS)$_8$PcCu				
Col_{ro2} (P2m) at 115 °C	*a* = 35.0	35.0	35.0	(1 0 0)
	b = 27.5	21.6	21.6	(1 1 0)
	h = 3.99	15.9	14.8	(2 1 0)
	Z = 1.0 for ρ = 1.1	10.8	10.7	(3 1 0)

(*Continued*)

Table 4. (*Continued*)

Compound (mesophase)	Lattice constants/Å	Spacing/ Å		Miller indices (*h k l*)
		Observed	Calculated	
		7.06	7.00	(5 0 0)
		6.58	6.41	(2 4 0)
		5.14	5.25	(2 5 0) + #2
		4.69	4.70	(7 2 0) + #2
		3.99	3.99	(0 0 1)[h]
1f: (*m*-C_{10}OPhS)$_8$PcCu				
Col_{ro1} (P2m) at 80 °C	*a* = 36.6	36.6	36.6	(1 0 0)
	b = 27.2	21.8	21.8	(1 1 0)
	h = 4.01	13.7	13.6	(0 2 0)
	Z = 0.98 for ρ = 1.1	10.7	10.9	(2 2 0)
		6.93	7.07	(5 1 0)
		5.01	4.98	(5 4 0) + #2
		4.61	4.57	(8 0 0) + #2
		4.01	4.01	(0 0 1)[h]
Col_{ro2} (P2m) at 115 °C	*a* = 37.0	37.0	37.0	(1 0 0)
	b = 27.6	22.1	22.1	(1 1 0)
	h = 4.06	10.6	11.1	(2 2 0)
	Z = 1.0 for ρ = 1.1	7.06	7.15	(5 1 0)
		5.08	5.05	(5 4 0) + #2
		4.61	4.60	(0 6 0) + #2
		4.06	4.06	(0 0 1)[h]
1g: (*m*-C_{12}OPhS)$_8$PcCu				
Col_{ro2} (P2m) at 100 °C	*a* = 39.5	39.5	39.5	(1 0 0)
	b = 21.3	21.3	21.3	(0 1 0)
	h = 5.09	10.7	10.7	(0 2 0)
	Z = 0.97 for ρ = 1.1	8.02	7.90	(5 0 0)
		6.98	7.00	(1 3 0)
		5.09	5.09	(0 0 1)[h]
		4.63	—	#2
Col_{ro1} (P2m) at 90 °C	*a* = 43.1	43.1	43.1	(1 0 0)
	b = 21.6	21.6	21.6	(0 1 0)
	h = 4.96	13.7	13.7	(3 0 0)
	Z = 1.1 for ρ = 1.1	10.8	10.8	(4 0 0)
		7.04	7.11	(1 3 0)
		4.96	4.96	(0 0 1)[h]
		4.62	—	#2
1h: (*m*-C_{14}OPhS)$_8$PcCu				
Col_{ro2} (P2m) at 105 °C	*a* = 43.7	43.7	43.7	(1 0 0)
	b = 21.5	21.5	21.5	(0 1 0)
	h = 5.08	14.4	14.6	(3 0 0)
	Z = 1.0 for ρ = 1.1	10.6	10.7	(0 2 0)

(*Continued*)

Table 4. (*Continued*)

Compound (mesophase)	Lattice constants/Å	Spacing/ Å		Miller indices (*h k l*)
		Observed	Calculated	
		7.14	7.15	(0 3 0)
		5.08	5.08	(0 0 1)[h]
		ca. 4.6	—	#2
Col_{ro1} (P2m) at 85 °C	a = 50.1	50.1	50.1	(1 0 0)
	b = 22.6	22.6	22.6	(0 1 0)
	h = 4.59	14.3	13.4	(3 1 0)
	Z = 1.1 for ρ = 1.1	10.7	11.0	(4 1 0)
		7.09	7.16	(7 0 0)
		ca. 4.9	—	#2
		4.59	4.59	(0 0 1)[h]
1i: (m-C_{16}OPhS)$_8$PcCu				
Col_{ro1} (P2m) at 100 °C	a = 49.9	49.9	49.9	(1 0 0)
	b = 28.6	24.8	24.8	(1 1 0)
	h = 4.07	17.0	16.6	(3 0 0)
	Z = 1.0 for ρ = 1.0	10.7	10.8	(3 2 0)
		7.07	7.07	(1 4 0)
		ca. 5.1	—	#2
		ca. 4.6	—	#2
		4.07	4.07	(0 0 1)[h]

#1, #2 = broad halos due to the thermal fluctuation of the phenylthio groups and the molten alkyl chains, respectably. h = stacking distance. ρ = assumed density (g/cm^3). * [20].

seen from these photos, photo (a) shows a focal conic texture typical of liquid crystalline phases and photo (b) shows a dendritic texture typical of a hexagonal columnar (Col_h) phase. Therefore, this liquid crystalline phase of **1b** could be identified as a Col_h phase. Photo (c) is a Col_{ro2}(P2m) phase in the moderately long alkyl-substituted derivative (m-C_{10}OPhS)$_8$PcCu (**1f**) at 115 °C. Both (d) and (e) are a Col_{ro1}(P2m) phase in the same derivative **1f** at 90 °C. As can be seen from these photos, both $Col_{ro1,2}$ phases did not give any typical textures of mesophases. However, when the phase in photo (d) was pressed and sheared, it showed both stickiness and birefringence as shown in photo (e). Therefore, the Col_{ro1}(P2m) phase in **1f** could be identified as a liquid crystalline phase. Photo (f) shows a Col_{ro1}(P2m) phase in the longest alkoxy-substituted derivative (m-C_{16}OPhS)$_8$PcCu (**1i**) at 100 °C. This photo exhibits a focal conic texture typical of liquid crystalline phases. In addition, when this sample was pressed and sheared, it showed both stickiness and birefringence as shown in photo (g). Therefore, this phase could be also identified as a liquid crystalline phase.

Temperature-dependent small angle X-ray diffraction (TD-SAXS) measurements

Table 4 summarizes temperature-dependent small angle X-ray diffraction (TD-SAXS) data of the liquid crystalline phases in (m-C_nOPhS)$_8$PcCu (**1a~1i**). Figures 4, 5 and 6 show the representative SAXS patterns of (m-C_2OPhS)$_8$PcCu (**1b**), (m-C_{10}OPhS)$_8$PcCu (**1f**) and (m-C_{16}OPhS)$_8$PcCu (**1i**), respectively. In these figures, the enlarged diffractgrams are shown as the insets. These SAXS patterns were measured for the samples obtained by cooling from isotropic liquid.

The SAXS pattern of (m-C_2OPhS)$_8$PcCu (**1b**) at 220 °C is shown in Fig. 4. As can be seen from this figure, a very broad halo (#1) due to thermal fluctuation of phenylthio groups was observed in 2Θ = 13~23°. This broad halo #1 was also observed for the previous flying-seed-like liquid crystalline derivative, (m-C_1OPhS)$_8$PcCu (**1a**) [20]. The d-spacings in the low angle region are in a ratio of 1:1/√3:1/√7:1/3, which is typical of a Col_h phase. Therefore, the mesophase could be identified as a Col_h phase. This identification is consistent with the dendritic

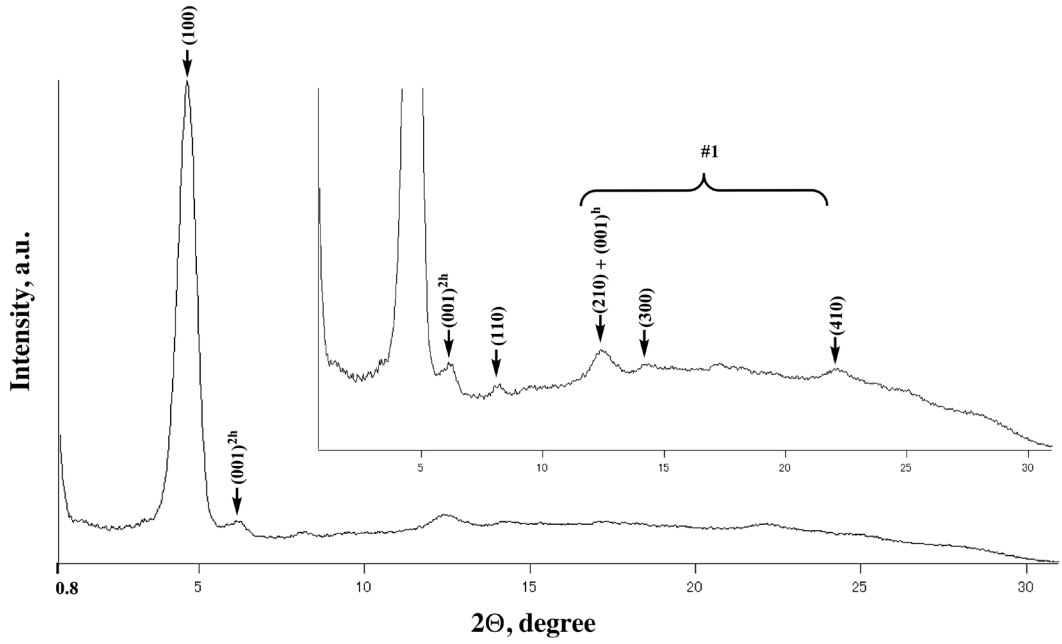

Fig. 4. XRD pattern of (m-C_2OPhS)$_8$PcCu (**1b**) at 220 °C (on cooling from I.L). #1 = broad halo due to the thermal fluctuation of the phenylthio groups

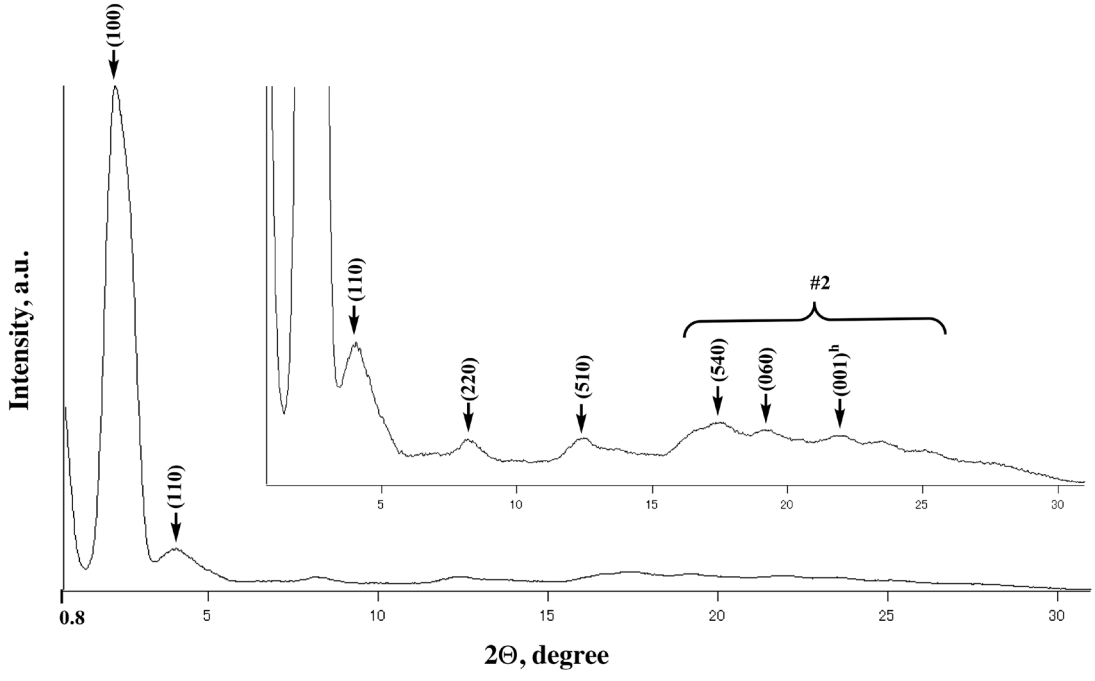

Fig. 5. XRD pattern of (m-C_{10}OPhS)$_8$PcCu (**1f**) at 115 °C. #2 = broad halo due to the molten alkyl chains

texture typical of a Col_h mesophase mentioned above. In addition, two peaks at around 2Θ = 6° and 13° could be assigned to the interdimer stacking d_{001}(2h = 14.3 Å) and the intermonomer stacking d_{001}(h = 7.12 Å), respectively. This means that an equilibrium between the dimers and monomers exists in the Col_{ho} mesophase as the same case as the [m,p-(C_nO)$_2$PhO]$_8$PcCu derivatives reported in 2001 [7]. From the Z value calculation [40], the Z value of this Col_{ho} mesophase in **1b** could be obtained as Z = 1.0 assuming the intermonomer stacking distance as h = 7.12 Å and the density of the mesophase as ρ = 1.0 g.cm^{-3}. Although the intracolumnar stacking distance h (7.12 Å) is much larger than that of conventional Col_{ho} phases. However, the value Z = 1.0 is consistent with the theoretical

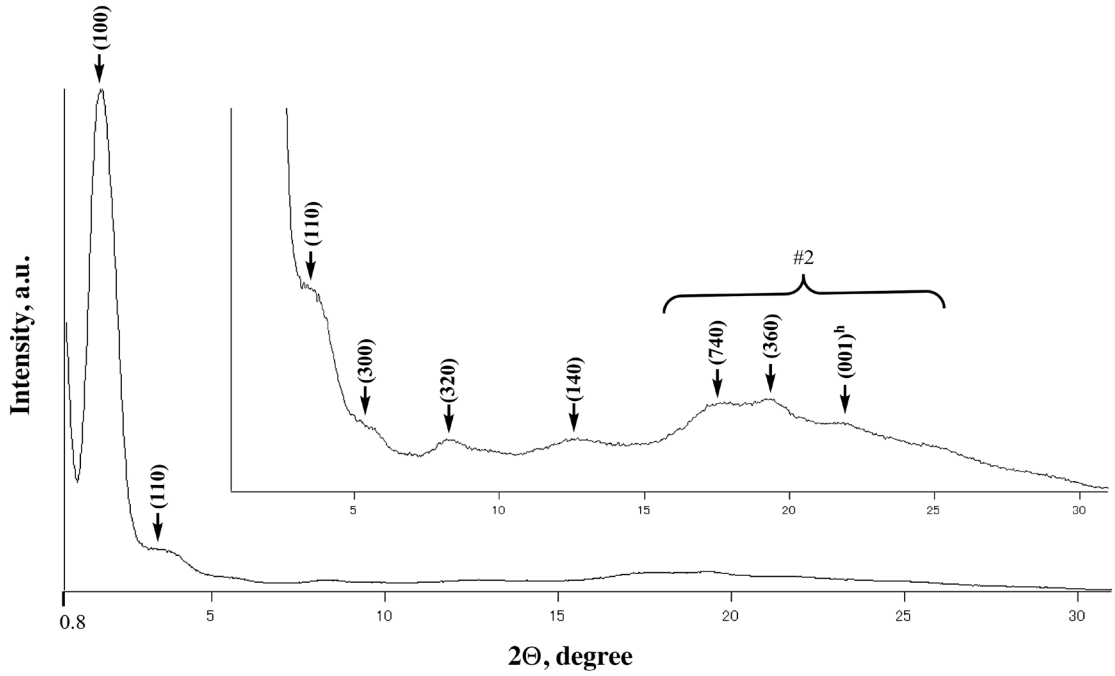

Fig. 6. XRD pattern of (m-$C_{16}OPhS)_8PcCu$ (**1i**) at 100 °C (on cooling from I.L). #2 = broad halo due to the molten alkyl chains

value ($Z = 1.0$) for a Col_{ho} mesophase. Moreover, the large stacking distance h = 7.12 Å is comparable to that of flying-seed-like liquid crystals reported in our previous works [20, 24]. Thus, the present derivative **1b** could be classified as a flying-seed-like liquid crystal similar to the previously reported derivative **1a**. In our previous work, this liquid crystalline phase of **1a** was identified as a Col_{ro}(P2m) phase [20]. However, the d spacings of **1a** are also in a ratio of $1:1/\sqrt{3}:1/\sqrt{7}:1/3$, the same as that of **1b**. From the Z value calculation, the result ($Z = 0.95 \fallingdotseq 1.0$) is consistent with a Col_{ho} phase. Moreover, the equilibrium between the dimers and monomers in the Col_{ho} mesophase could be also observed as the same case as the (m-$C_2OPhS)_8PcCu$ (**1b**) homolog. Therefore, the liquid crystalline phase of **1a** could be also identified as Col_{ho} phase, so that we correct the identification of this mesophase from Col_{ro}(P2m) to Col_{ho} in this study.

Figure 5 shows a SAXS pattern of the moderately long alkoxy-substituted derivative (m-$C_{10}OPhS)_8PcCu$ (**1f**) at 115 °C. As can be seen from this figure, a broad halo (#2) due to the molten long alkyl chains was observed. From the reciprocal lattice calculation [40], the liquid crystalline phase was identified as Col_{ro2} (P2m) (a = 37.0 Å, b = 27.6 Å, h = 4.06 Å). Figure 6 shows the SAXS pattern of the longest alkoxy-substituted derivative (m-$C_{16}OPhS)_8PcCu$ (**1i**) at 100 °C. The liquid crystalline phase was also identified as Col_{ro1}(P2m) (a = 49.9 Å, b = 28.6 Å, h = 4.07 Å). It is very interesting that each of the present longer alkoxy-substituted *phenylthio* derivatives (m-$C_nOPhS)_8PcCu$ (n = 4~16) showed only *rectangular* columnar (Col_{ro}(P2m)) phase (s), whereas each of the previous longer alkoxy-substituted *phenoxy* derivatives (m-$C_nOPhO)_8PcCu$(n = 10~20) showed only a *hexagonal* columnar (Col_{ho}) phase [8, 9].

Columnar stacking structures of (m-$C_nOPhO)_8PcCu$ (n = 10–20) and (m-$C_nOPhS)_8PcCu$ (n = 1–16)

The different mesophase appearance mentioned above may be attributed to difference of interaction among the Pc cores having steric hindrance of the peripheral substituents (PhO and PhS).

It is well-known that stronger interaction between cores is required to form a rectangular columnar (Col_r) phase in comparison with a hexagonal columnar (Col_h) phase [41–43]. As schematically shown in Fig. 7, covalent bond radius of sulfur atom (1.04 Å) is larger than that of oxygen atom (0.66 Å). Hence, C–S bond length (1.81 Å) is longer than C–O bond length (1.43 Å) [44]. Accordingly, the interaction between Pc cores in the *phenoxy*-substituted derivatives (m-$C_nOPhO)_8PcCu$ (n = 10–20) is weakened by bigger steric hindrance of the *phenoxy* groups closer to the Pc core. As the result, the *phenoxy*-substituted derivatives (m-$C_nOPhO)_8PcCu$ (n = 10–20) may form the hexagonal columnar phase (Col_h). On the other hand, the interaction between Pc cores in the *phenylthio*-substituted derivatives (m-$C_nOPhS)_8PcCu$ (n = 4–16) is strengthened by smaller steric hindrance of phenylthio group farther from the Pc core. In this case, an additional coordination bonds may be formed between copper atoms and nitrogen atoms between the upper and lower Pc cores, as illustrated

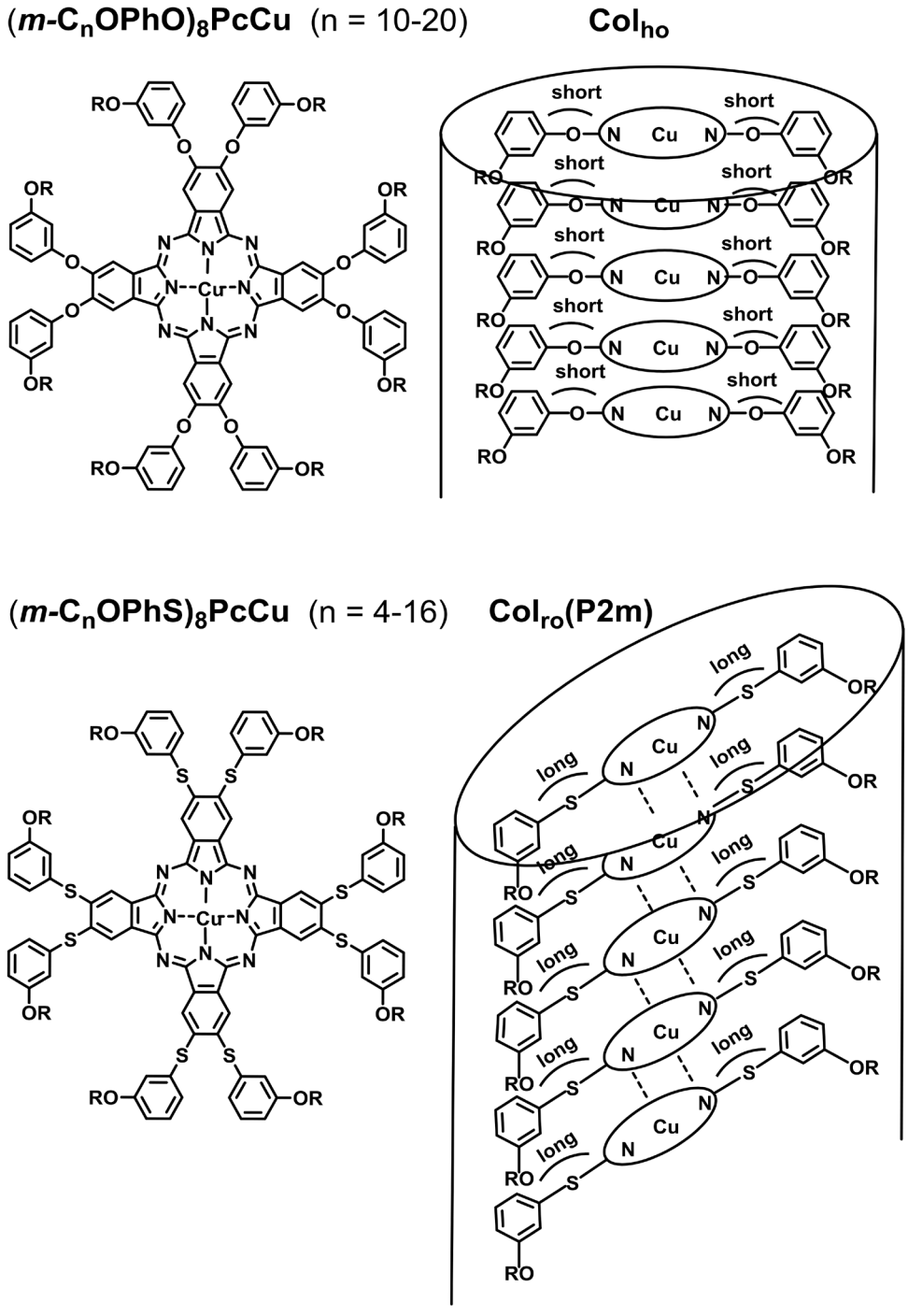

Fig. 7. Columnar stacking structures of (m-C_nOPhO)$_8$PcCu (n = 10–20) and (m-C_nOPhS)$_8$PcCu (n = 4–16)

in Fig. 7 (dotted lines). Thus, the *phenylthio*-substituted derivatives (m-C_nOPhS)$_8$PcCu (n = 4–16) may form the rectangular columnar (Col_r) phase.

UV-vis absorption spectra

Figure 8 shows the UV-vis absorption spectra of (m-C_{10}OPhO)$_8$PcCu (upper) and (m-C_{10}OPhS)$_8$PcCu (**1f**) (lower) in THF solution. Table 5 lists their spectral data. As can be seen from these figure and table, the Q-band of the *phenylthio*-substituted derivative (m-C_{10}OPhS)$_8$PcCu (**1f**) red-shifts by 35.7 nm into near infrared region compared with the *phenoxy*-substituted derivative (m-C_{10}OPhO)$_8$PcCu. This result is compatible with those of the *phenylthio*-substituted phthalocyanes reported so far [16–20].

Moreover, we could estimate the optical band gaps of (m-C_{10}OPhO)$_8$PcCu and (m-C_{10}OPhS)$_8$PcCu (**1f**) from absorption edge of the Q-bands to be 1.79 eV and 1.70 eV, respectively. Hence, the *phenylthio*-substituted

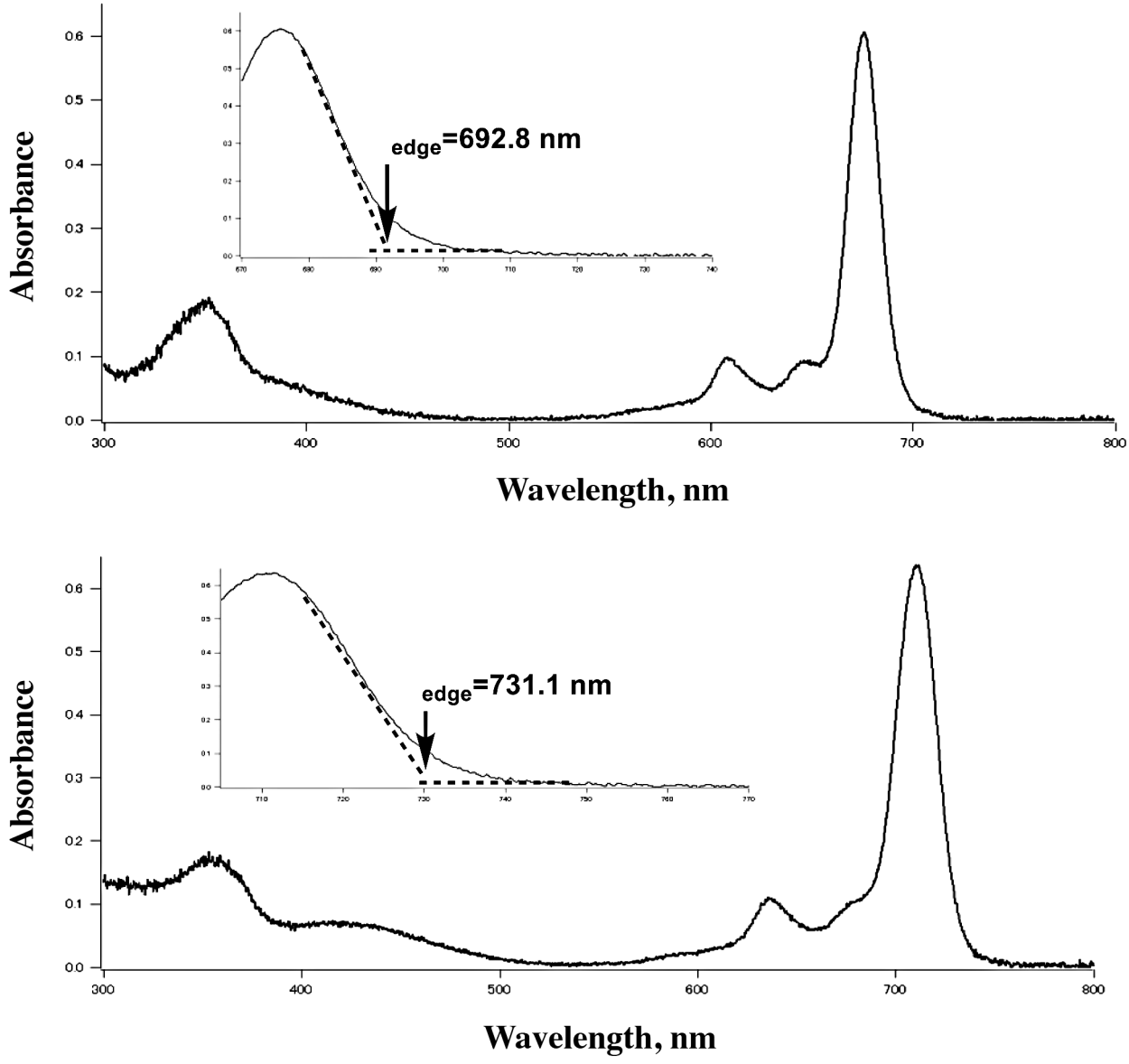

Fig. 8. UV-vis absorption spectra of (*m*-C_{10}OPhO)$_8$PcCu (upper) and (*m*-C_{10}OPhS)$_8$PcCu (**1f**) (lower) in THF solution

Table 5. UV-vis spectral data of (*m*-C_{10}OPhO)$_8$PcCu and (*m*-C_{10}OPhS)$_8$PcCu in THF solution

Compound	Concentration ($X10^{-6}$mol L^{-1})	λ_{abs}/nm (logε)			λ_{edge}/nm	E_{gap}*/eV
		Soret band	Q-band			
			Q_{0-1}-band	Q_{0-0}-band		
(*m*-C_{10}OPhO)$_8$PcCu	2.27	351.9 (4.93)	608.3 (4.64)	675.9 (5.43)	692.8	1.79
(*m*-C_{10}OPhS)$_8$PcCu (**1f**)	2.29	353.3 (4.90)	635.7 (4.69)	711.6 (5.44)	731.1	1.70

* E_{gap} was estimated from the absorption edge of Q-band.

derivative gave a narrower band gap by *ca.* 0.1 eV in comparison with the *phenoxy*-substituted derivative.

CONCLUSION

In this study, we have successfully synthesized novel phenylthio-substituted phthalocyanine derivatives (*m*-C_nOPhS)$_8$PcCu (**1b~1i**) to reveal their mesomorphism. We found that the shortest alkoxy-substituted derivatives, (*m*-C_1OPhS)$_8$PcCu (**1a**) and (*m*-C_2OPhS)$_8$PCu (**1b**) could be classified as flying-seed-like liquid crystals. On the other hand, the other longer alkoxy-substituted derivatives (*m*-C_nOPhS)$_8$PcCu: n = 4~16 (**1c~1i**) could be classified as conventional long alkyl-chain-melting liquid crystals. It is very interesting that each of the present longer alkoxy-substituted *phenylthio* derivatives (*m*-C_nOPhS)$_8$PcCu (n = 4~16) showed only *rectangular* columnar (Col_{ro}-(P2m)) phase(s), whereas each of the previous longer alkoxy-substituted *phenoxy* derivatives (*m*-C_nOPhO)$_8$PcCu (n = 10~20) showed only a *hexagonal* columnar (Col_{ho}) phase. The different mesophase appearance may be originated from the difference of interaction among the Pc cores having steric hindrance of the peripheral substituents (PhO and PhS). The Q-band of the *phenylthio*-substituted derivative (*m*-C_{10}OPhS)$_8$PcCu (**1f**) red-shifts by 35.7 nm into near infrared region compared with the *phenoxy*-substituted derivative (*m*-C_{10}OPhO)$_8$PcCu. Thus, in this study, we successfully synthesized a novel series of liquid crystalline (*m*-C_nOPhS)$_8$PcCu (n = 1~16) derivatives showing the Q-bands in near infrared region. We intend to measure the charge carrier mobilities in the near future.

REFERENCES

1. Chandrasekhar S, Sadashira BK and Suresh KA. *Pramana* 1977; **9**: 471–480.
2. Cammidge AN and Bushby RJ. *Handbook of Liquid Crystals*, Vol. 2B, Wiley-VCH: 1998; Chap. 7, pp. 693–743.
3. Sergeyev S, Pisula W and Geerts YH. *Chem. Soc. Rev*. 2007; **36**: 1902–1929.
4. Ban K, Nishizawa K, Ohta K and Shirai H. *J. Mater. Chem.* 2000; **10**: 1083–1090.
5. van de Craats AM, Shouten PG and Warman JM. *Ekisho*, 1998; Vol. 2, no. 1.
6. Warman JM, Kroeze JE, Schouten PG and van de Craats AM. *J. Porphyrins Phthalocyanines* 2003; **7**: 342–350.
7. Hatsusaka K, Ohta K, Yamamoto I and Shirai H. *J. Mater. Chem.* 2001; **11**: 423–433.
8. Ichihara M, Suzuki A, Hatsusaka K and Ohta K. *J. Porphyrins Phthalocyanines* 2007; **11**: 503–512.
9. Sato H, Igarashi K, Yama Y, Ichihara M, Itoh E and Ohta K. *J. Porphyrins Phthalocyanines* 2012; **16**: 1148–1158.
10. Kandaz M, Yılmaz İ and Bekaroğlu Ö. *Polyhedron* 2000; **19**: 115–121.
11. Balakireva OV, Maizlish VE and Shaposhnikov GP. *Russ. J. Gen. Chem*. 2003; **73**: 292–296.
12. Kobayashi N, Ogata H, Nonaka N and Luk'yanets EA. *Chem. Eur. J.* 2003; **9**: 5123–5134.
13. Lu G, Bai M, Li R, Zhang X, Ma C, Lo P-C, Ng DKP and Jiang J. *Eur. J. Inorg. Chem.* 2006; 3703–3709.
14. Arican D, Arici M, Uğur AL, Erdoğmus A and Koca A. *Electrochimica Acta* 2013; **106**: 541–555.
15. Mayukh M, Lu C-W, Hernandez E and McGrath DV. *Chem. Eur. J*. 2011; **17**: 8427–8478.
16. Polaske NW, Lin H-C, Tang A, Mayukh M, Oquendo LE, Green J, Ratcliff EL, Armstrong NR, Saavedra SS and McGrath DV. *Langmuir* 2011; **27**: 14900–14909.
17. Yu L, Shi W, Lin L, Guo Y, Li R and Peng T. *Dyes Pigm.* 2015; **114**: 231–238.
18. Shi W, Peng B, Guo Y, Lin L, Peng T and Li R. *J. Photochem. Photobiol., A* 2016; **321**: 248–256.
19. Zimcik P, Malkova A, Hruba L, Miletin M and Novakova V. *Dyes Pigm.* 2017; **136**: 715–723.
20. Ishikawa A, Ohta K and Yasutake M. *J. Porphyrins Phthalocyanines* 2015; **19**: 639–650.
21. Ohta K, Shibuya T and Ando M. *J. Mater. Chem.* 2006; **16**: 3635–3639.
22. Takagi Y, Ohta K, Shimosugi S, Fujii T and Itoh E. *J. Mater. Chem*. 2012; **22**: 14418–14425.
23. Hachisuga A, Yoshioka M, Ohta M and Itaya T. *J. Mater. Chem. C* 2013; **1**: 5315–5321.
24. Yoshioka M, Ohta K and Yasutake M. *RSC Adv.* 2015; **5**: 13828–13839.
25. Watarai A, Ohta K and Yasutake M. *J. Porphyrins Phthalocyanines* 2016; **20**: 822–832.
26. Barluenga S, Dakas P-Y, Ferandin Y, Meijer L and Winssinger N. *Angew. Chem. Int. Ed*. 2006; **45**: 3951–3954.
27. Patent PCT/US2006/041501.
28. Hwang JY, Arnold LA, Zhu F, Kosinski A, J. Mangano T, Setola V, Roth BL and Guy RK. *J. Med. Chem.* 2009; **52**: 3892–3901.
29. Wakioka M, Ikegami M and Ozawa F. *Macromolecules* 2010; **43**: 6980–6985.
30. Jiang Y, Qin Y, Xie S, Zhang X, Dong J and Ma D. *Org. Lett.* 2009; **11**: 5250–5253.
31. Natarajan P, Sharma H, Kaur M and Sharma P. *Tetrahedron. Lett.* 2015; **56**: 5578–5582.
32. Patel SK and Long TE. *Tetrahedron. Lett.* 2009; **50**: 5067–5070.
33. Wöhrle D, Eskes M, Shigehara K and Yamada A. *Synthesis* 1993; 194–196.
34. Kamiyama T, Enomoto S and Inoue M. *Chem. Pharm. Bull.* 1985; **33**: 5184–5189.
35. Newman MS and Karnes HA. *J. Org. Chem.* 1996; **31**: 3980–3984.
36. Itoh T and Mase T. *Org. Lett.* 2004; **6**: 4587–4590.

37. Itoh T and Mase T. *J. Org. Chem.* 2006; **71**: 2203–2206.
38. Mazzio KA, Okamoto K, Li Z, Gutmann S, Strein E, Glinger DS, Sclaf R and Luscombe CK. *Chem. Commun.* 2013; **49**: 1321–1323.
39. Heine NB and Studer A. *Macromol. Rapid. Commun.* 2016; **37**: 1494–1498.
40. (a) Ohta K. *Dimensionality and Hierarchy of Liquid Crystalline Phases: X-ray Structural Analysis of the Dimensional Assemblies*, Shinshu University Institutional Repository, submitted on 11 May, 2013; http://hdl.handle.net/10091/17016. (b) Ohta K. In *Identification of discotic mesophases by X-ray structure analysis*, *Introduction to Experiments in Liquid Crystal Science* (*Ekisho Kagaku Jikken Nyumon* [*in Japanese*]), Japanese Liquid Crystal Society, Sigma Shuppan: Tokyo, 2007; Chap. 2-(3), pp. 11–21, ISBN-13:978-4915666490.
41. Laschat S, Baro A, Steinke N, Giesselmann F, Hägele C, Scalia G, Judele R, Kapatsina E, Sauer S, Schreivogel A and Tosoni M. *Angew. Chem. Int. Ed.* 2007; **46**: 4832–4887.
42. Zheng H, Lai CK and Swager TM. *Chem. Mater.* 1995; **7**: 2067–2077.
43. Morale F, Date RW, Gullion D, Bruce DW, Finn RL, Wilson C, Blake AJ, Schröder M and Donnio B. *Chem. Eur. J*. 2003; **9**: 2484–2501.
44. Atkins PW and de Paula J. *Physical Chemistry,* 8th edition, 2006.
45. Watarai A, Ohta K and Yasutake M. *J. Porphyrins Phthalocyanines* 2016; **20**: 1444–1456.

